Article

Case Study in Modular Lightweight Steel Frame Construction: Thermal Bridges and Energy Performance Assessment

Bojan Milovanović [1], Marina Bagarić [1,*], Mergim Gaši [1] and Nikolina Vezilić Strmo [2]

1   Department of Materials, Faculty of Civil Engineering, University of Zagreb, 10000 Zagreb, Croatia
2   Independent Chair for Buildings, Faculty of Civil Engineering, University of Zagreb, 10000 Zagreb, Croatia
*   Correspondence: marina.bagaric@grad.unizg.hr

Abstract: This paper proposes an improvement of the conventional Lightweight Steel Frame (LSF) wall structure suitable for the design of high-performance modular buildings. A mobile module, named MUZA, is used as a case study building to analyse the performance of such LSF structures in terms of their thermal bridging effect on the *U*-value of the opaque envelope elements, linear heat losses at junctions, and moisture condensation risk, as well as thermal bridging effect on the overall energy performance of the building. The study included an additional climate- and orientation-dependent analysis that examined the performance of MUZA under various conditions. The main conclusion is that the steel studs increase the *U*-value from 28.4% to 41.6% compared to cases without the studs, which consequently increases transmission losses through opaque elements. Thanks to the continuous covering of the metal studs with thermal insulation, the thermal bridges at the element junctions are minimized, and in almost all cases, the Ψ-values are well below 0.1 W/(m·K) and are free from moisture condensation. The overall impact of thermal bridges on heating energy demand is significant, while the impact on cooling energy is less pronounced. The designed module with the proposed LSF wall structure can meet the Croatian requirements for Nearly Zero-Energy Buildings (NZEB), but the shading devices and photovoltaics orientation must be optimized depending on the climatic conditions and the orientation of the large transparent openings. MUZA can be a promising solution for post-disaster housing, providing better indoor environmental quality, healthy living conditions, and low energy bills for the affected people. In addition, it can also be used for permanent housing when a fast and robust modular construction is required which is also energy efficient and sustainable.

Keywords: modular construction; lightweight steel frame building; Nearly Zero-Energy Building; thermal bridge; energy performance; numerical simulations; thermal transmittance

1. Introduction

Recent earthquake events in Southern Europe (Italy [1,2], Albania [3], Greece [4], Turkey [5], or Croatia [6]) revealed similar issues of the vulnerability of building stock [7] in all the aforementioned countries. Analysing only the recent earthquakes in Croatia, after the Zagreb earthquake, some 25,000 buildings were damaged, the majority of them in the city centre, while after the Petrinja earthquake, some 56,000 were damaged, mainly in rural areas. A total of 4621 buildings were rendered unusable due to damage [8]. The World Bank estimated the total financial costs of the damage from the Zagreb earthquake at EUR 11.3 billion and EUR 5.5 billion for the Petrinja earthquake [9,10].

These devastating events resulted in the need to quickly take care of a large number of people, i.e., to find them temporary and/or permanent residence, as well as to return their usual lives to "normal" as quickly as possible (shops, hospitals, kindergartens, etc.), not to mention establishing places of work for the people. Unfortunately, it turned out that the applied modular solutions were not adequate, because they mainly included conventional construction site containers in which it is impossible to live in the summer (overheating)

but also in the winter (cold, excessive surface condensation, and mould growth), and they are huge consumers of energy. At the same time, such modular constructions are unsafe for life due to bad and overloaded installations (fires due to electrical installations) [11].

Emergency housing units, such as temporary buildings, are thought to be appropriate solutions to meet the needs of the earthquake-affected population for a medium period of time (approx. two years) during which damaged buildings can be rebuilt or repaired [12]. For this purpose, modular buildings have a wide variety of uses as both temporary (relocatable) and permanent structures. Modules are produced in standard sizes and shapes, and can then be assembled on site into buildings with many repetitive units or can be assembled into more advanced architecture.

The module must also be flexible to operate as a single and self-sufficient building or, exploitable as a part of cluster of several modules to form larger building. This paper will deal with the possibility to use module as a single self-sufficient building with the useful floor area less than 50 m^2.

For the temporary buildings and stand-alone buildings with a useful floor area less than 50 m^2, the EPBD II Directive [13] states in Article 4 that Member States may decide not to set or apply the minimum energy performance requirements for several categories of buildings, among which temporary buildings with a time of use of two years or less are mentioned. This article was then transposed to Croatian legislation [14] as well as in Italian legislation [12], meaning that temporary buildings used in emergencies are not required to comply with minimum energy performance or emissions of the building.

In the Italian case, this proved to be a significant setback, since after numerous seismic events that have struck Italy, the use of emergency housing units, as well as temporary schools, etc., has exceeded two years. In the case of the L'Aquila earthquake in 2009, some of the temporary structures are still used in 2022 [12]. In case of earthquakes that struck Croatia in 2020, it is now clear in mid-2022 that the temporary buildings erected will be in use for a substantially longer period than two years. In addition, people living in temporary housing in Croatia are receiving very high utility bills for electricity (used for heating and cooling), the fire safety is at risk, and there are issues with condensation of water vapour in their temporary units. Thus, it is clear that the energy efficiency and building physics of these temporary buildings are of crucial importance in order to ensure the comfort and health of the occupants, as well as to ensure minimum utility expenses to people who have lost their homes or places of work in the areas where energy infrastructure is often damaged.

Regardless of the construction system used for the building envelope, including the Lightweight Steel Frame (LSF), it must be designed to ensure indoor environmental quality and very low energy consumption in all different climatic conditions in which it can be used.

Furthermore, except in such extraordinary situations, there is an increasing demand on the market in general for prefabricated and modular construction of residential, public, and commercial buildings.

Buildings that can provide comfort to occupants and very low energy consumption are known as Nearly Zero-Energy Buildings (NZEB), which are defined in [13] as buildings with very high energy performance. This "nearly zero" amount of energy needed for heating and cooling is to be covered to a very significant extent by the energy from renewable sources produced on-site or nearby. The commission's proposal to revise the directive from December 2021 [15] makes a step forward from the current NZEB to zero-emission buildings (ZEB), aligning the energy performance requirement for new buildings to the longer-term climate neutrality goal and "energy efficiency first principle." According to the Commission's proposal, a ZEB is defined as a building with a very high energy performance, with the very low amount of energy still required fully covered by energy from renewable sources at the building, district, or community level [15].

All the above considered, the NZEB as well as future ZEB levels will force designers to rethink the constructive details so that their buildings will comply with the requirements,

without increasing the construction costs over an optimum level, but at the same time reducing greenhouse gas emissions [16].

Regarding the emissions of the buildings, when performing a life cycle analysis (LCA) of a building, it is vital to evaluate embodied and operational emissions as well as primary energies. In order to reduce the environmental impact, it is essential to reduce both emissions and energies from production, operation, and end of life phases. This paper will focus only on the operational energy related to the heating and cooling energy needs and the impact of the thermal bridges caused by the LSF elements in the building envelope. Nevertheless, it needs to be emphasized here that one should not exaggerate the thickness of thermal insulation in order to minimize the operational energy of buildings. It was shown in [17] that there is an optimal insulation thickness, which takes into account operational as well as embodied energy combined with the economic parameters.

Since LSF is not conventional, but is, rather, quite a scarce construction system to date in Croatia, the building physics and energy efficiency aspects have not been studied in depth considering southern European climate conditions. Thus, the main goal of this paper is to investigate whether the newly proposed LSF structure can meet high-performance requirements, such as the Croatian national requirements for NZEB, and to what extent thermal bridges, which are unavoidable due to the metal structure, affect the energy performance. In addition, this will show whether the newly proposed LSF module can be used for purposes including, but not limited to, temporary buildings, such as high-performance emergency housing units after natural disasters, which implies providing occupants with a high level of indoor thermal comfort, a healthy environment (moisture-free construction details), and very low energy consumption.

The paper is structured as follows. Section 2 provides a review of the literature on the conventional LSF structures currently available on the construction market, identifying its advantages and disadvantages. The newly proposed LSF structure, which is the subject of this paper, is also presented in the same section. Section 3 describes a case study of a building which implemented the newly proposed LSF structure, and is used for calculations in the next section. Section 4 outlines the methodology used for this research, including the description of methods used for the effective thermal transmittance, thermal bridge and building energy performance calculations, the description of analysed cases, and the assumptions used for the calculations. Section 5 presents calculation results. Section 6 offers conclusions and presents plans for future work.

2. Literature Review

Lightweight Steel Frame (LSF) buildings have now been accepted in the global construction industry [18–20], and are proving to be one of the construction systems suitable for building NZEBs [16]. This is due to the characteristics of the LSF structures, such as the rapid on-site construction; possibility of prefabrication; architectural flexibility; low weight with reasonably high load bearing capacity (possible to create spans of 6 m and room height of 4 m [21]); considerable possibility of recycling and reuse; reduced costs of labour, transportation, and installation; cost efficiency, etc. [16,19,22]. The LSF system is utilising thin-walled cold-formed profiles, most often U, K, C, and Z, with a wall thickness of 0.6 to 2.5 mm [21].

From an economic point of view, the LSF system offers benefits due to the obvious reduction of the construction time, the durability of the employed materials and the lighter foundations (as it is a lightweight construction system) [23].

It is reported in [24] that LSF reduces the labour costs from 62.5% up to 73%, while at the same time improving construction site logistics and operations, as well as management of consumables, operations, and logistics at the construction sites. The same research [24] reports a 50–86.7% reduction in the mass of waste when using LSF, and a significant reduction of 79.0–93.5% in the volume of water used when compared to the traditional system (depending on the case study analysed). Additionally, it is well known that steel has near 100% reuse rates [23] which deserves to be underlined, and this enables

a lower environmental impact at the end of the lifecycle for the majority of the generated construction and demolition waste.

All of these are significant LSF system advantages with regard to the "European Green Deal: achieving zero net emissions by 2050" [25,26]. Furthermore, LSF systems can offer a superior alternative when considering housing solutions or shelters in remote regions, or in case of natural disasters like earthquakes [27].

On the other hand, LSF structures have some drawbacks which should not be disregarded. For example, if not correctly addressed (optimised) during the design phase, 2D thermal bridges due to steel elements in walls, floors, roofs, etc., and especially 3D thermal bridges in the corners where three building elements connect, can result in increased heat losses [20,22]. This will, of course, lead to increased energy consumption of LSF buildings, as well as an increased risk of surface water vapour condensation and mould growth at thermal bridge locations, due to lower surface temperature. Roque and Santos [23] showed a very large variation in the insulation effectiveness due to its positioning in the LSF walls, with a direct consequence on their thermal transmittance (U or U-value). The authors of [23] showed that neglecting the effect of heat transfer in steel structures can underestimate the U-value by up to 94.73%. Similarly to these findings, de Angelis and Serra [28] also found differences up to 101%. It can, thus, be seen that thermal bridges created by the extensive use of steel can, in reality, penalize buildings' thermal envelope as well as their overall energy balance.

In order to minimize the risk of water vapour condensation within the layers of LSF structures, one needs to adopt one of the two following strategies: either to build a diffusion open structure or to reduce the amount of water vapour entering and propagating through the layers of the building envelope. The first option requires avoiding the possibility of having any steel members with a temperature below dew point. The other strategy would require vapour barriers on the interior side of the LSF structure.

In both ways, LSF structures as well as any other NZEBs or passive houses should have airtight building envelopes in order to reduce the ventilation heat losses, reduce the risk of condensation, ensure indoor air quality, eliminate drafts and improve comfort, improve noise insulation of building components, and retain efficiency of the ventilation system. On the other hand, a breathable but wind-tight layer located on the wall exterior should be installed to reduce the impact of wind on the performance of the insulation layer. Both airtightness and wind-tightness require attention and must be optimised in the design stage.

Furthermore, being lightweight and thinner than conventional building envelope elements, LSF structures have lower thermal inertia, thus reducing the possibility of passive energy storage in the building envelope and decreasing the overheating problems in buildings with high internal gains, or, on the other hand, increasing the summer overheating risk, especially in southern European climates [29]. Despite generally resulting in a more versatile indoor thermal environment in case of LSF, the analysis in [29] showed that lower thermal inertia of LSFs may have benefits considering the intermittent occupancy of the building.

Regarding the load-bearing properties, the main disadvantage of this system is that individual profiles are usually unable to transfer loads independently, so two or more profiles must be connected to each other, and only then do they form a load-bearing panel. Therefore, the performance is more sensitive to imperfections related to dimensions, and in terms of budget, proving sufficient resistance is much more complex [21].

LSF structures can be classified into three types [23,30], depending on the position of the thermal insulation: (a) cold frame construction; (b) warm frame construction; (c) hybrid frame construction (Figure 1).
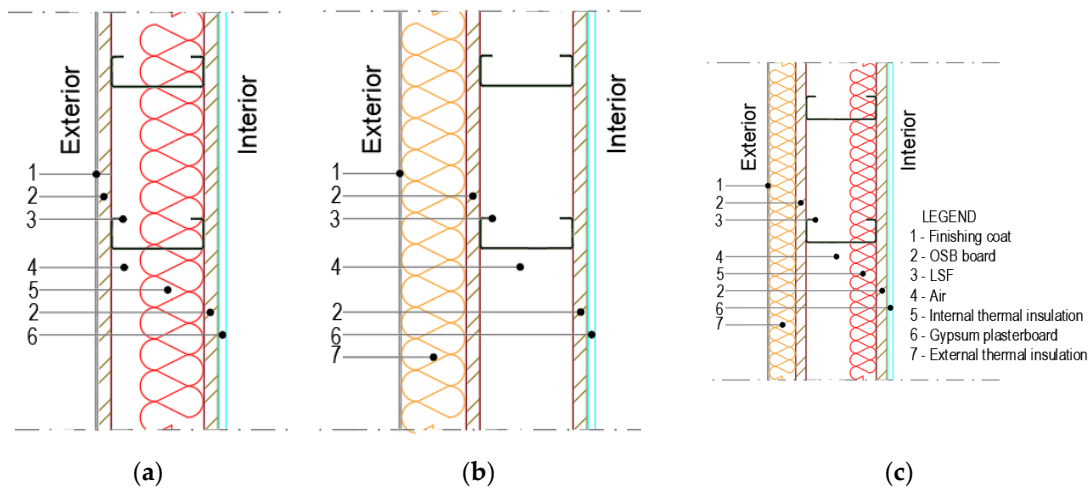
Figure 1. Classification of LSF structures: (**a**) cold frame construction; (**b**) warm frame construction; (**c**) hybrid frame construction.

In conclusion, each type of LSF structure has their advantages and drawbacks. The common drawback would be the difficulty to achieve airtight layer, keeping in mind that one needs to run installations (electrical, water, sewage, and possibly heating, cooling, ventilation, etc.) through the structure. The other deficiency of the LSFs shown in Figure 1 would be free moving air, which would increase heat losses due to convection within the LSF structure.

In order to avoid the issues of inadequate airtightness and freely moving air, this paper proposes the further development of existing LSF typology (Figure 2) by introducing the installation layer from the inside with two-fold function: (i) to enable continuity of airtight membrane with minimal penetrations, and (ii) easier access to installations. Moreover, by filling the entire thickness of the structure with thermal insulation, one avoids convection due to free air circulating (Figure 2).
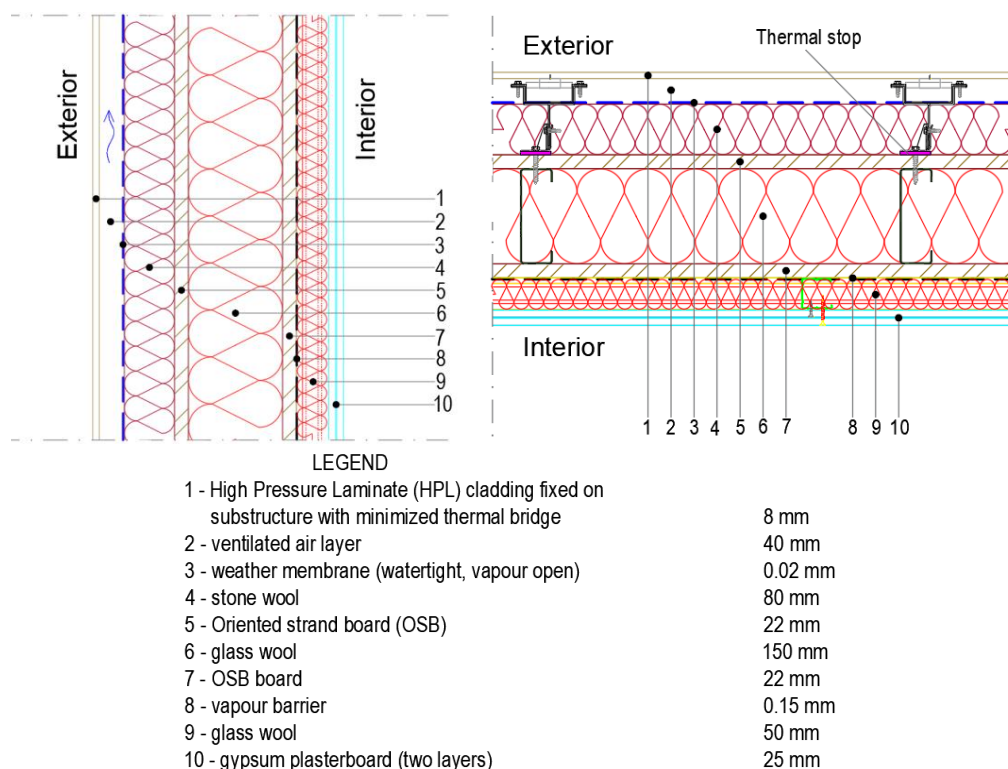

LEGEND

1 - High Pressure Laminate (HPL) cladding fixed on substructure with minimized thermal bridge	8 mm
2 - ventilated air layer	40 mm
3 - weather membrane (watertight, vapour open)	0.02 mm
4 - stone wool	80 mm
5 - Oriented strand board (OSB)	22 mm
6 - glass wool	150 mm
7 - OSB board	22 mm
8 - vapour barrier	0.15 mm
9 - glass wool	50 mm
10 - gypsum plasterboard (two layers)	25 mm

Figure 2. Proposed LSF wall structure (**left**—vertical cross-section; **right**—horizontal cross-section).

This newly proposed LSF structure is considered to have significantly improved thermal behaviour compared to conventional LSF structures; however, extensive calculations should be performed in order to evaluate its performance. Therefore, the influence of thermal bridges on the thermal behaviour of the building envelope elements, but also on the energy consumption of the entire building, is investigated using the example of a single module with a useful floor area of less than 50 m^2. This paper presents the study of 2D thermal bridges, in which proposed LSF walls (Figure 2) meet other building elements, such as a corner between two walls or a junction with the floor, roof, and a window. Secondly, the research is focused on whether the proposed LSF design approach can reach the NZEB levels as prescribed in the Croatian legislation [14] and simultaneously fulfil the EU targets. Furthermore, the aim of this work is to conduct an additional parametric analysis on case study building, in order to determine the dependence of the building's energy consumption on the climatic location and the orientation of the building itself.

3. The Case Study

The case study of the LSF building is a mobile pavilion called MUZA (in Croatian, *Mobilna, Učinkovita, Zdrava, Arhitektura*, which translates to English as *Mobile, Efficient, Healthy, Architecture*), realized within the framework of the EU Horizon 2020 project "The NZEB Roadshow" [31,32]. MUZA is a single module designed to function as a demonstration building of NZEB systems and technologies, with the intention of placing it in public areas and allowing visits from anyone interested. However, even though MUZA is designed for this specific use, it is conceived to be modular and flexible, in order to allow easy adaptation for other possible uses, i.e., emergency housing units, permanent housing, kindergartens, schools, shopping centres, offices, etc.

3.1. Design Requirements and Architecture

The crucial requirement for the MUZA was the transportability of the building; therefore, during the design of the building, the reference was made to the dimensions of 9 m shipping container, as they are transportable on all major roads using a semi-truck. This ensures the mobility of MUZA as well as its use in different locations and in different climatic conditions. Another important aspect was the speed of construction and possibility of using already trained workers. From these, it was evident that at least three different construction systems with dry construction process are feasible, namely cross-laminated timber (CLT) panels, timber-frame, and LSF systems. Due to the lack of competency of construction workers in Croatia to construct CLT, as well as high material prices and the need to import the panels, CLT structure was rejected. On the other hand, the ability to find large quantities of material easily on the market, as well as the availability of competent metal workers in Croatia (a large number of manufacturers on the market are able to meet the requests with no special machinery) and higher rigidity of metal structures, steered the design of MUZA towards the LSF system.

The second crucial requirement for the design of the MUZA was to pay particular attention to minimizing heating and cooling energy needs, and to ensure the highest possible indoor environment quality.

The MUZA (Figures 3 and 4) has floor plan dimensions of 9.00 × 3.00 m and height 3.25 m (on flatbed truck under 4.20 m) which are within the dimensions allowed for road freight.
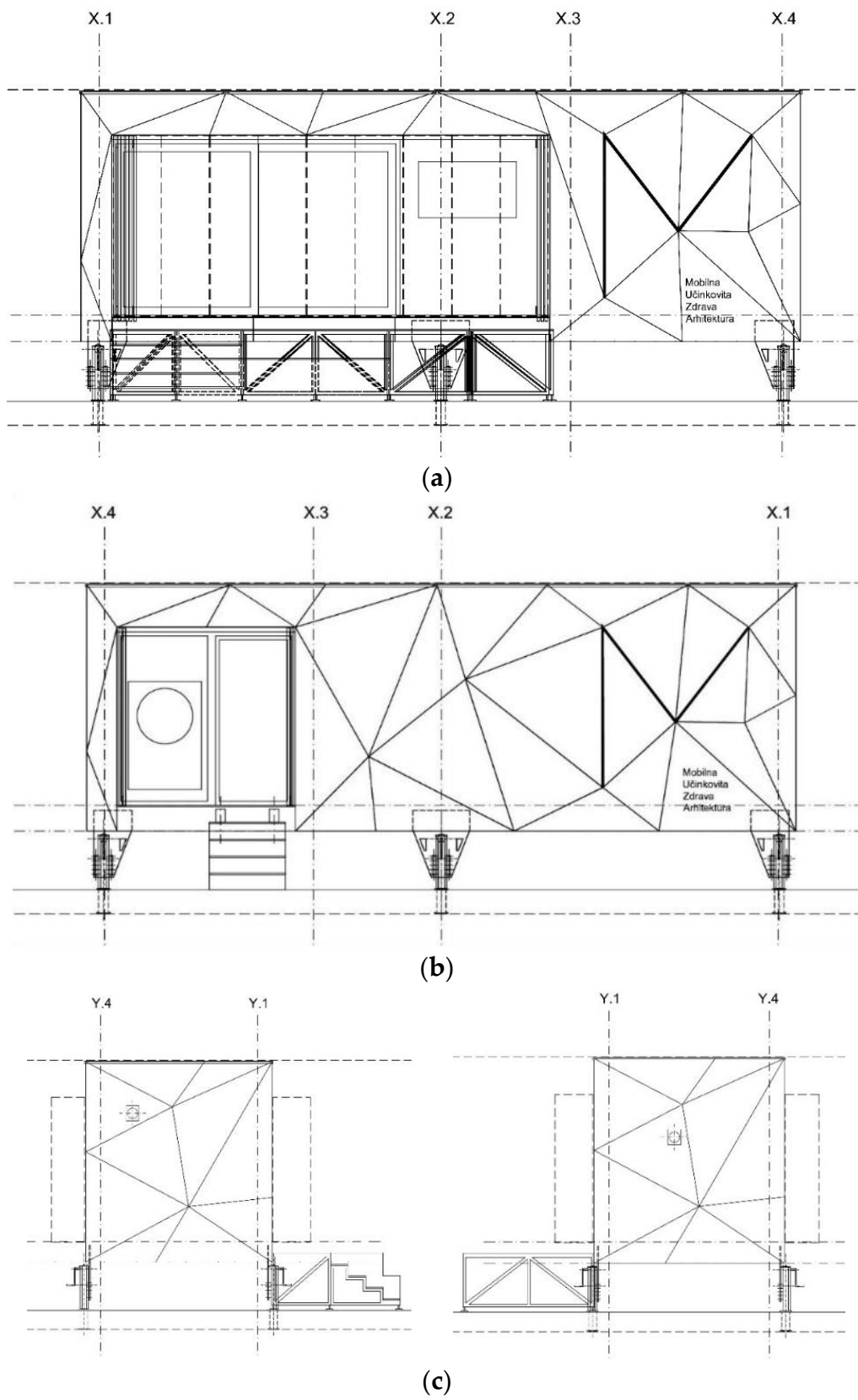
(**a**)

(**b**)

(**c**)

Figure 3. Exterior views of the MUZA pavilion: (**a**) main façade, (**b**) back façade, (**c**) side façades.

Figure 4. View of the main façade of the MUZA constructed with the LSF system.

Table 1 presents the basic geometric characteristics of the MUZA used in energy balance modelling.

Table 1. Geometric characteristics of the MUZA.

Net floor area, A_k [m^2]	14.75
Gross floor Area, A_f [m^2]	22.35
External surface area of the building envelope, A [m^2]	118.96
Heated building gross volume, V_e [m^3]	69.73
Heated air volume, V [m^3]	35.84
Shape factor, f_0 [m^{-1}]	1.71

3.2. Structural Design and Building Envelope Characteristics

The loadbearing structure is LSF (Figure 5), on which six steel sheets are welded and used as removable landing gears, which are then used to transfer forces to the ground (Figure 4). The wall has a single layer of vertical steel studs every 600 mm, while in exceptional situations where additional stiffening is needed, or for load bearing purposes, the gap between two vertical studs is 300 mm. In case of floor studs, the gap between two studs is 380 mm, while the gap between the roof studs is 480 mm (Figure 5). These distances were determined in a structural analysis, taking into account ultimate limit states and especially serviceability limit states, which was dominant due to the limit of maximum deflections of the glazing, technical systems installed, and aesthetics (cracking of internal surfaces, etc.).

Non-combustible thermal insulation (mineral wool) is placed between vertical (wall) and horizontal (floor and roof) steel studs, while continuity of thermal insulation is maintained by adding additional thermal insulation to both the external and internal side of the walls, roof, and floor. Different physical–mechanical properties of mineral wool insulation are required depending on the building envelope element in which it is installed (filling between steel studs, external insulation in the ventilated air cavity, additional thermal insulation layer under gypsum plasterboards). Depending on this, and in consultation with the manufacturers, different types of mineral wool insulation were selected (stone or glass wool). All characteristic layers of opaque building envelope elements are shown in Figure 6.
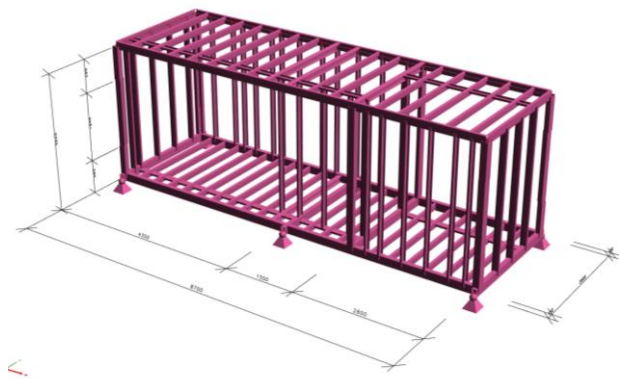
Figure 5. Load bearing steel structure of the MUZA: **left**—numerical model, **right**—realized structure.
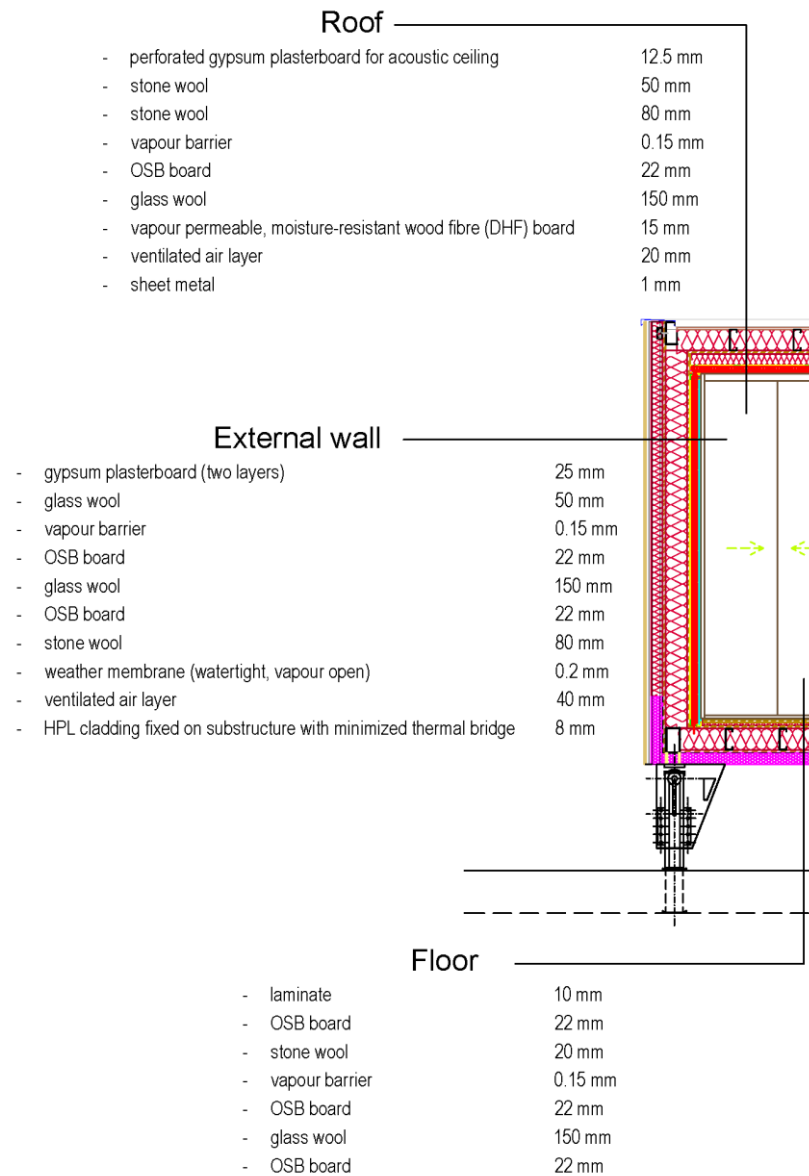

Figure 6. MUZA's opaque envelope assemblies.

Two sliding doors are placed on the main and back façade, respectively, and are characterized by triple glazing with low-e coating, argon filling, and PVC profile. On the main façade, larger sliding doors (3.7 × 2.2 m) have external and internal safety glazing (precaution measures due to the facts that the MUZA will be publicly used and frequently transported).

Calculated thermal transmittance for larger sliding doors is U_w = 0.83 W/m^{2}K (U_g = 0.6 W/m^{2}K, U_f = 1.1 W/m^{2}K, $g_\perp$ = 0.60), and U_w = 0.97 W/m^{2}K (U_g = 0.7 W/m^{2}K, U_f = 1.3 W/m^{2}K, $g_\perp$ = 0.70) for smaller sliding doors (2.3 × 2.2 m), respectively.

As it was expected that large transparent elements on a building with a small useful floor area and indoor air volume would lead to overheating issues and thermal discomfort, three levels of shading were foreseen:

i.　*Window shutters on both sliding doors acting as a lateral shading*—during transport, they are closed, and their primary function changes to protecting the glazing from mechanical damage caused by external factors (rocks, birds, etc.).

ii.　*Venetian blinds on larger sliding doors*—motorized blinds can be manually controlled through a central unit, but they can be programmed to start shutting down automatically when solar radiation is too strong, or at sunset.

iii.　*Self-load bearing textile overhang on larger sliding doors*—this can be easily removed and installed when needed.

Airtightness of the building envelope was achieved by applying a vapour barrier and by properly sealing all penetrations and sliding doors. Prior to the installation of gypsum plasterboards, airtightness was tested using the Blower Door method to detect potential leakages and improve the quality of the works. Keeping in mind that n_{50} (air changes per hour at 50 Pa) greatly depends of the building volume [33], it is considered that parameter q_{E50} (volume of air flowing through the m^2 of envelope at 50 Pa pressure difference) is more relevant, i.e., a more realistic airtightness indicator, for the MUZA's small volume. Based on Blower Door testing, airtightness of the MUZA's envelope is q_{E50} = 1.25 m^3/h·m^2.

3.3. Technical Systems and Monitoring

Due to the small volume of the MUZA and the high level of airtightness of the thermal envelope, it was necessary to install mechanical ventilation with heat recovery (MVHR) in order to ensure adequate indoor air quality. MVHR is realized by two units of a decentralized MVHR system, which, at the same time, allows for saving energy. The efficiency of the installed heat recovery system is 80%.

The heating and cooling needs are met by a highly efficient air-to-water reversible heat pump (heating and cooling power 5 kW, *COP* up to 4.93 for +A7/W35, according to EN 14825). Heated or cooled indoor air is distributed by two fan coil units. One unit is located in the suspended ceiling directly above the technical room, while another unit is located on the wall (Figure 7).

Three photovoltaic (PV) panels of total nominal power output 1.005 kWp, are installed on the roof. Their inclination can be manually adapted in range from 15–45° (Figure 4). When the PV panels are inclined, they have the same orientation as the main façade. Therefore, PV's orientation is related to the position of the MUZA itself in a certain location. The idea was to use the electricity generated by the PVs only for the MUZA's ongoing needs (HVAC, lighting, mechanical ventilation, TV, tablets, sensors for monitoring, etc.), i.e., to be energy self-sufficient when outdoor conditions make it possible. Moreover, due to mobility requirements and related administration issues, it was not an option to release excess energy to the grid. Therefore, a smart inverter was chosen as the optimal solution. The smart inverter is actually "smart" thanks to a system-compatible component Energy Meter, which calculates phase-exact and balanced electrical measured values, and communicates these via Ethernet to the local network. In this way, all produced and used electricity can be communicated to the system frequently and with a high level of precision. In this way, no excess electricity is produced. When weather conditions are unfavourable, the required difference of electricity is taken from the grid.
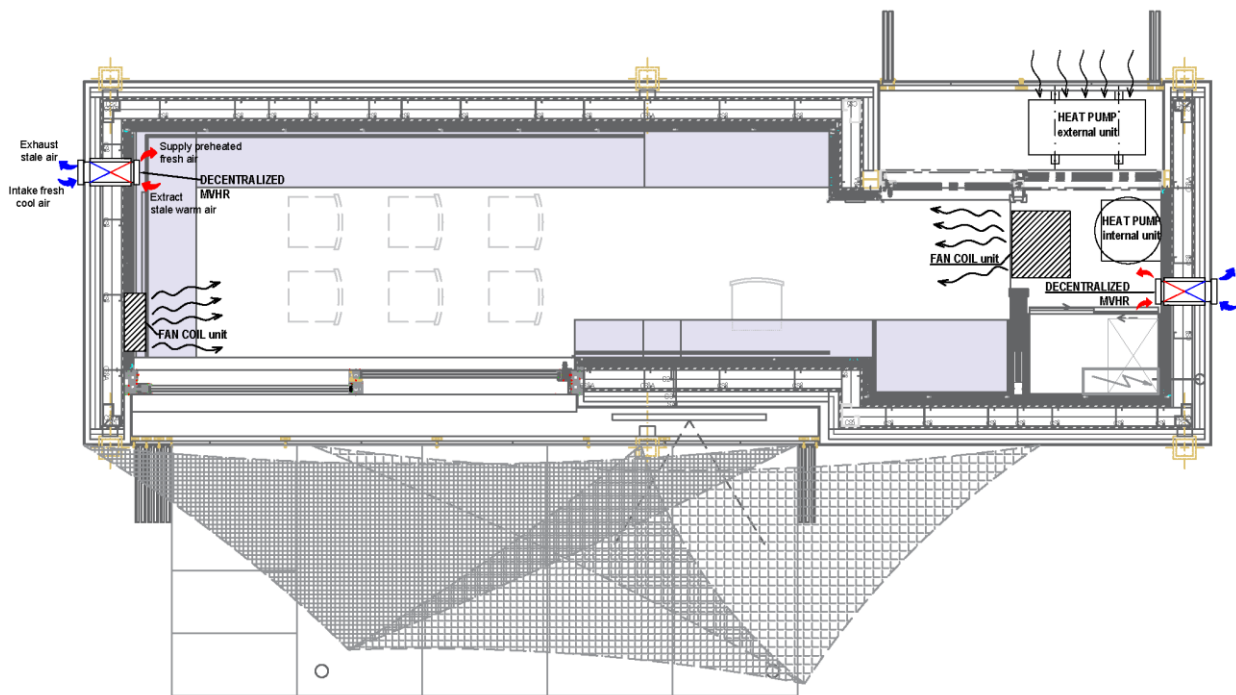
Figure 7. Floor plan with position of technical systems.

A real-time monitoring system is installed in order to understand how MUZA performs when used in real conditions and in different climates, where monitored parameters are the following: energy consumption, energy produced by PV panels, indoor air quality parameters (temperature, relative humidity, CO_2 concentration, relative indoor air quality), and hygrothermal performance of the external wall (temperature and relative humidity in all characteristic layers).

The system measures energy consumption of the whole building, HVAC system, MVHR and ventilation system, and lighting. Energy consumption is measured using smart WiFi modules (power tags) that monitor and measure energy and power in real-time (current, voltage, power, power factor, energy) and wirelessly communicate these data via a gateway to the router. Power tags are installed on the classical automatic fuses. This home automation is controlled using a logical controller (gateway) installed in the main distribution cabinet. Monitoring is out of the scope of this paper, and the results will be analysed and published elsewhere.

4. Research Methodology

Figure 8 summarizes the research methodology used in this paper. Each step is described in detail in the following subsections.

4.1. Materials and Boundary Conditions

The building envelope's materials used in this study, with their thickness and basic hygrothermal characteristics (thermal conductivities λ and water vapour diffusion resistance factor μ), are shown in Table 2.

Table 2. Building envelope assemblies—material thickness and basic hygrothermal properties.

| Building Element	Layer (Internal to External)	Thickness [cm]	λ [W/m·K]	μ [-]
EXTERNAL WALL	Gypsum plasterboard	1.25	0.25	8
	Gypsum plasterboard	1.25	0.25	8
	Glass wool	5	0.037	1.10
	Vapour barrier	0.015	0.50	230,000
	Oriented strand board (OSB) board	2.20	0.13	50
	Glass wool	15	0.035	1.10
	OSB board	2.20	0.13	50
	Stone wool	8	0.034	1.10
	Weather barrier (watertight, vapour open)	0.20	0.50	5
	Intensively vented air layer	4	contribution neglected	contribution neglected
	HPL cladding	0.80	contribution neglected	contribution neglected
ROOF	Gypsum plasterboard	1.25	0.25	8
	Stone wool	5	0.035	1.10
	Stone wool	8	0.035	1.10
	Vapour barrier	0.015	0.50	230,000
	OSB board	2.20	0.13	50
	Glass wool	15	0.032	1.10
	DHF board	1.50	0.10	11
	Weakly vented air layer	2	0.30	1
			0.12	1
	Sheet metal	0.05	50	1,000,000
FLOOR	Laminate	1	0.13	50
	OSB board	2.20	0.13	50
	Stone wool	2	0.036	1.10
	Vapour barrier	0.015	0.50	230,000
	OSB board	2.20	0.13	50
	Glass wool	15	0.035	1.10
	OSB board	2.20	0.13	50
	Bitumen waterproofing	0.50	0.23	50,000
	Extruded Polystyrene (XPS)	8	0.034	140
Additional	**Description**		**λ [W/m·K]**	**μ [-]**
Steel	For LSF and perimeter columns and beams		50	1,000,000
Polyvinyl Chloride (PVC)	Window subframe		0.57	50,000
air_gap_1	Chamber in the windowsill		0.14	1
air_gap_2	Chamber in the windowsill		0.28	1
air_gap_3	Chamber in the windowsill		0.17	1
air_gap_4	Chamber in the windowsill		0.43	1
Window	Window		0.165	50,000
Window insulation	Thermal insulation around window subframe		0.038	1.10
Air in steel column	Air in reinforced vertical support and drainage pipe (corner of two walls)		0.6812	1
Air in steel beam	Beam support around the perimeter of the floor		0.5456	1
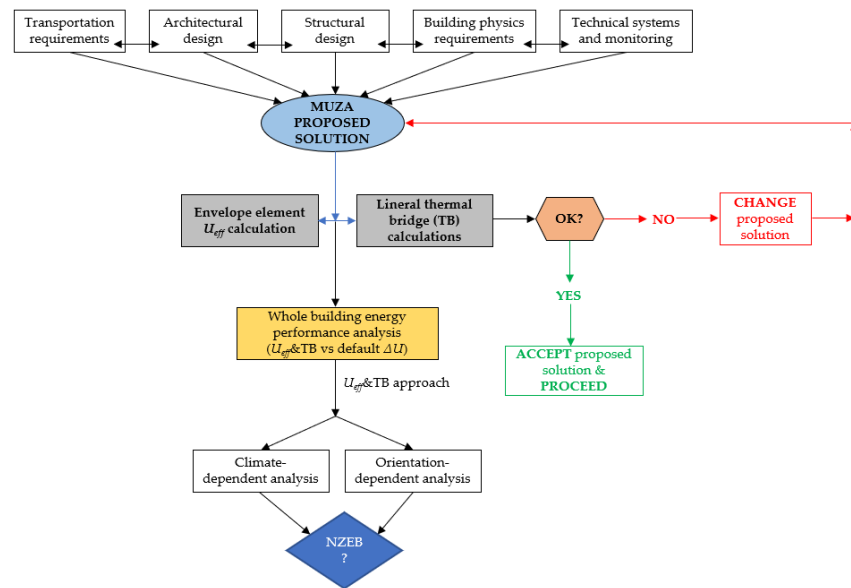
Figure 8. Graphical representation of the research methodology.

The contribution of an intensively vented air layer in the external wall to the thermal resistance of the entire wall was disregarded. Modelling of other air layers inside the thermal envelope (roof, window subframe, drainage pipe, etc.) was performed using EN ISO 6946 [34], considering the equivalent thermal conductivity of a solid (Table 2). Additionally, the vapour barrier, weather barrier, and waterproofing layer were ignored as per recommendation from [35] for layers with a thickness less than 1 mm.

Regarding the surface heat transfer coefficients needed for numerical calculations, they were taken according to [34]. The values of these coefficients, depending on the type of surface (external or internal) and the heat flow direction, are shown in Table 3. The same boundary conditions were used across the whole paper.

Table 3. Surface heat transfer coefficients [34].

Heat Flux Direction	Boundary	h [W/(m^{2}K)]
Horizontal	Exterior	25.00
	Interior	7.69
Upwards	Exterior	25.00
	Interior	10.00
Downwards	Exterior	25.00
	Interior	5.88

Boundary conditions set for the external and internal environment are shown in Table 4, and they are in line with EN ISO 10211 [35]. The temperature of the external environment ($-10°$C) also corresponds to the air temperature of the coldest day in the continental climate of Croatia.

Table 4. Air temperature and relative humidity values.

Air	T [°C]	RH [%]
Exterior	−10.00	90.00
Interior	−20.00	60.00

4.2. Calculation of Effective Thermal Transmittance

The building's thermal envelope may have thermally homogeneous or heterogeneous layers, and the accurate estimation of heat losses of structures with studs and thermal insulation is of vital importance for reliable calculation of the building's energy needs [20].

The European standard EN ISO 14683 [36] does not consider the contribution of thermal bridges in LSF walls, making it impossible to estimate the contribution of thermal bridges to the heat losses using the tabulated values. Even though the EN ISO 6946 [34] standard provides a simplified method for calculating thermal resistance of a building component consisting of homogeneous and heterogeneous layers, the situations with steel studs cannot be calculated using this simplified method, due to the significant difference between the upper and lower resistance values [16], and only a numerical calculation is admissible [37].

Approaches to an estimation of thermal transmittance (*U*-value) or thermal resistance (*R*-value) of heterogeneous layers are described in detail in [20], where the analytical method according to EN ISO 6946 [34], or its adaptation of the method by Gorgolewski [38], can be used. Furthermore, ASHRAE Zone Method [39] and its numerical approach could be used to assess these thermal bridges [35] using 2D or 3D models for point thermal bridges (i.e., joints between horizontal and vertical elements, etc.). In addition to the evaluation of heat losses, critical temperatures in the critical positions can also be checked using 2D and/or 3D numerical models.

In this paper, two-dimensional (2D) models are used to perform a calculation of the effective *U*-value of the MUZA's opaque elements, which represent its characteristic thermal envelope components with integrated steel studs. Four cases, as shown in Table 5 and Figure 9, were analysed in total—walls with steel studs spacing between 60 cm and 30 cm, the roof with steel studs spacing of 48 cm, and the floor with steel studs spacing of 38 cm. Steel stud spacings are defined based on static calculations. The *U*-values predicted by the numerical calculations were calculated by employing the approach described in EN ISO 10211-1 [35]. Cross-sections of the representative wall, floor, and roof are shown in Figures 6–9. The layers and their properties are shown in Figure 6 and Table 2, respectively.

Each wall, floor, and roof comprises a steel structure containing cold-formed C-shaped steel studs (150 × 50 × 20 × 1.5 mm) welded to a steel frame which is formed by rectangular hollow steel sections (180 × 100 × 5 mm).

Two-dimensional numerical models resulted in the thermal transmittance of the overall structure, and an effective *U*-value (U_{eff}). U_{eff} [35] was derived from the two-dimensional thermal coupling coefficient L_{2D} [W/m·K], which essentially represents the overall heat transferred through the building element. If one determines the L_{2D} from the numerical model according to the [35] and divides it with the length of the geometrical model l, one can derive the U_{eff} value (Equation (1)).

$$U_{eff} = \frac{L_{2D}}{l} \qquad (1)$$

where the L_{2D} can be calculated as shown in Equation (2) [35], where ϕ [W/m] is the heat flow rate resulting from the 2D calculation, and T_i and T_e are the internal and external environment temperature, respectively.

$$L_{2D} = \frac{\phi}{(T_i - T_e)} \qquad (2)$$

The difference between the effective thermal transmission U_{eff} and the one-directional *U*-value is calculated according to Equation (3):

$$\Delta U = \frac{U_{eff} - U}{U} \cdot 100 \qquad (3)$$

Here, U is the thermal transmittance calculated according to the EN ISO 6946 [34] (Equation (4)).

$$U = \frac{1}{\frac{1}{h_{si}} + \sum_1^n \frac{d}{\lambda} + \frac{1}{h_{se}}} \tag{4}$$

where h_{si} and h_{se} are internal and external surface heat transfer coefficients, taken according to Table 3, and d and λ are thickness and thermal conductivity of the each of the n specific layers, respectively, taken according to Table 2.

The inverse of the thermal transmittance is the thermal resistance R. Thermal resistance is a measurement of a material's or a building element's resistance to heat flow. R is calculated according to Equation (5) [34].

$$R = \frac{1}{U} \tag{5}$$

Numerical analysis of heat transfer and calculation of L_{2D} is executed using CRORAL software [40], the in-house developed software based on the calculation procedures described in the EN ISO 10211 [35] and EN ISO 10077-2 [41]. CRORAL is validated by the current versions of these standards [40].

After calculating the L_{2D}, one can determine the linear thermal transmittance ψ-value using Equation 6 [35] for the evaluation of the contribution of the steel studs to the thermal transmittance and the evaluation of the quality of construction details from the thermal point of view.

$$\psi = L_{2D} - \sum_{i=1}^n U_i \times l_i \tag{6}$$

where U_i is the one-directional thermal transmittance of the i-th building element separating the two environments, and l_i is the length of the 2D geometrical model over which the U_i value is applied. The ψ-value was determined using the external dimensions.

The temperature factor f_{Rsi}, calculated according to Equation (7) [35], is of importance for well-being and comfort reasons. The f_{Rsi} is defined as the ratio between the minimum internal surface temperature ($T_{si,min}$) and the external air temperature (T_e) difference, and the average internal (T_i) and external (T_e) air temperature difference:

$$f_{Rsi} = \frac{T_{si,min} - T_e}{T_i - T_e} \tag{7}$$

The smaller ψ-value means that the additional heat losses through thermal brides are smaller, and the risk of construction damage such as mould growth is reduced. At the same time, a value of f_{Rsi} closer to 1 indicates a more uniform temperature distribution on the internal surface, i.e., that internal surface temperature is very close to indoor air temperature.

4.3. Thermal Bridge Numerical Simulations

Thermal bridges become critical as a proportion of total heat loss when the thermal transmittance of the building's envelope is reduced. In order to evaluate the building as a whole, in addition to the transmission heat losses through the respective building elements such as walls, roofs, floors, and windows, one needs to analyse the heat losses through all of their respective junctions. Hens recommends in [42] that thermal bridge impact should stay below $0.1 \times U$ in insulated and energy efficient buildings, and below $0.05 \times U$ in low energy buildings. Stricter requirements are in place for passive buildings where linear thermal transmittances Ψ should be lower than 0.01 W/(m K), while for window reveals 0.05 P_W/A_W is acceptable (P_W—window perimeter, A_W—window surface) [42].

Based on the detailed view of the building envelope shown in Figures 6 and 7, several characteristic construction details were identified as thermal bridges, such as: wall–wall corner, wall–niche, wall–floor connection, roof–wall connection, wall–sliding door frontal

connection, wall–sliding doors niche, sliding doors–wall side connection, sliding doors–floor connection, and sliding doors–roof connection. The geometrical models used for numerical calculations are presented in Figure 10.

Numerical analysis of heat transfer and calculation of L_{2D} is executed again using CRORAL software, based on the calculation procedures described in the EN ISO 10211 [35] and EN ISO 10077-2 [41].

In EN ISO 10211 [35], the modelling of complex components such as windows, doors, mullion and transom façades, etc., is not dealt with in detail. In principle, therefore, geometric simplifications are not permissible. The calculation of the ψ values in this paper was performed using the simplification in the geometric model by creating the replacement block with the U-value of the window, as described in [37]. In this case, a substitute block is formed with the frame width of the real window, which has an equivalent thermal conductivity that corresponds to the thermal resistance of the window.

4.4. Energy Performance Calculations—Thermal Bridge Incorporation Approach

Regarding the energy performance of the whole building, heating and cooling energy needs were calculated according to the simple hourly method described in standard EN ISO 13790 [43]. This calculation method was selected because it is the official calculation method in Croatia, prescribed by national legislation. Calculations were performed considering the primary function of the MUZA and with the interior air temperature T_i = 20 °C for the case of 4 climate conditions in Croatia (Gospić, Zagreb Maksimir, Split Marjan, and Hvar). All of the materials and building envelope characteristics were taken as shown earlier in this paper (Figure 6, Tables 1 and 2). All the elements of the building envelope were taken as having direct contact with external air (meaning no heat losses towards the ground). Geometric characteristics for all building elements were calculated using the overall external dimensions. Geometric characteristics of MUZA are shown in Table 1. Technical systems installed in MUZA are described in Section 3.3. Energy generated on an installed PV system was calculated according to the Croatian algorithm for determining energy requirements and efficiency of thermotechnical systems in buildings [44], adopted by the Croatian Ministry of Physical Planning, Construction and State Assets. All energy performance calculations were conducted with the assumption that the MUZA is not shaded by neighbouring buildings.

The climates of Gospić and Zagreb Maksimir can be classified as Cfb and Cfa climates, respectively, according to the Köppen-Geiger climate classification, while on the other hand, the climates of Split Marjan and Hvar are both classified as Csa climates according to the Köppen-Geiger climate classification. In order to quantify the demand for heating energy for a building, it may be better to use heating degree days (HDD) for the observed cities. HDD's are as follows: Gospić HDD = 3486.0, Zagreb Maksimir HDD = 3045.2, Split Marjan HDD = 1437.7, Hvar HDD = 1173.0. Only days with a daily mean air temperature equal to or below 15°C are considered for HDD.

In terms of energy performance, the specific heating ($Q''_{H,nd}$) and cooling energy ($Q''_{C,nd}$) needs were calculated, as well as the specific delivered energy (E''_{del}) and specific primary energy (E''_{prim}). Delivered energy (E''_{del}) included heating, and cooling energy, as well as energy generated on the PV system. The E''_{prim} was calculated using the primary energy factor of f_p = 1.61 for electrical energy.

During the analysis, the impact of thermal bridges was evaluated, where, firstly, thermal bridges were taken into account by using the default U-value increase (ΔU) prescribed in Croatian technical regulations [14]. This ΔU was taken with the value ΔU = 0.05 W/(m²K), which can also be found in the regulations of other EU member states for well insulated buildings. In the second variant, thermal bridges are taken into account by using the ψ-values listed in Table 6 with the respective lengths of the thermal bridges and the U_{eff}-values of the opaque envelope elements.

4.5. Parametric Study—Climate and Orientation Dependent Analysis

Additional analyses were conducted in this research regarding the energy performance of the MUZA, depending on the climate of the possible location as well as the orientation of the building. This ensures the mobility of the MUZA, its use in different locations and in different climatic conditions, and the specifics of the orientation on the location itself. As in the previous Section 4.4, four climate conditions in Croatia were analysed, namely Gospić, Zagreb Maksimir, Split Marjan, and Hvar. These climatic conditions were chosen in this analysis because Zagreb Maksimir and Split Marjan are the official reference meteorological stations for the continental and littoral climates of Croatia. On the other hand, Gospić and Hvar were chosen because they represent small cities with the highest and lowest HDD in Croatia, respectively. Orientation analysis was performed for the four cardinal directions (north, east, south, west), and the front façade with the larger transparent opening is considered the main façade (i.e., reference for orientation analysis).

5. Results and Discussion

This section represents the core findings of the analysed effect of thermal bridges on the 1D element level (effective thermal transmittance due to metal studs), the 2D element level (linear heat losses and risk of moisture condensation at junction details), as well as the 3D whole building level (energy performance). At the end, results of additional climate- and orientation-dependent analysis of the mobile module MUZA are presented.

5.1. Comparison between U and U_{eff}

The results of the effective thermal transmittance U_{eff} of opaque building elements from numerical calculations are presented in Table 5 and in Figure 9, together with the difference to the one-dimensional *U*-value, the linear thermal transmittance ψ contribution of the steel studs, and the temperature factor f_{Rsi}.
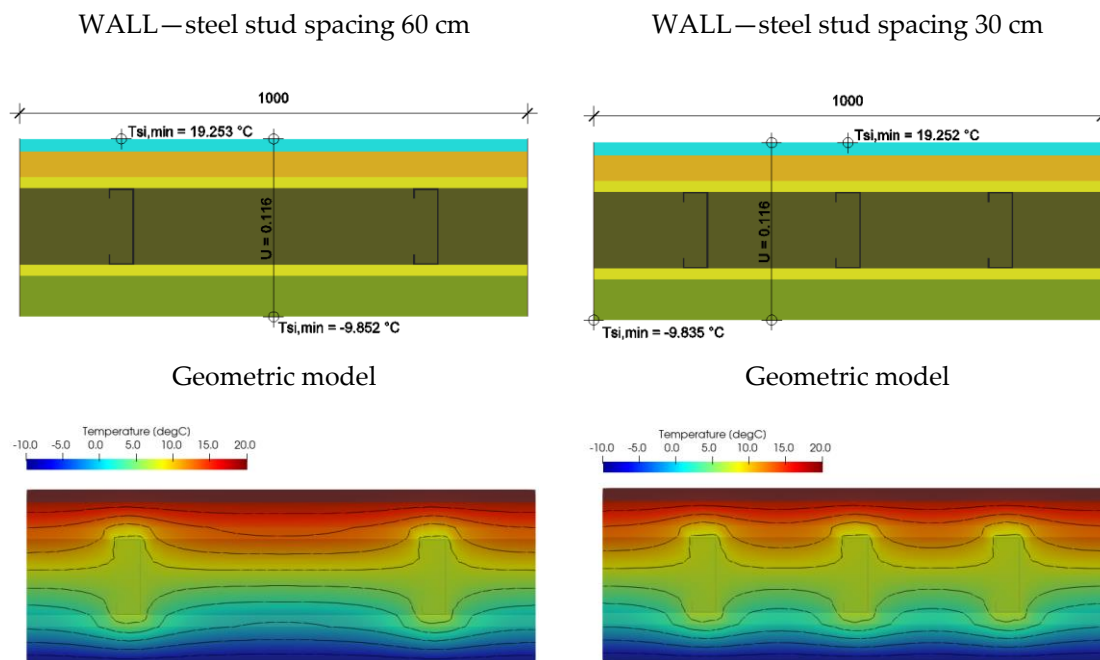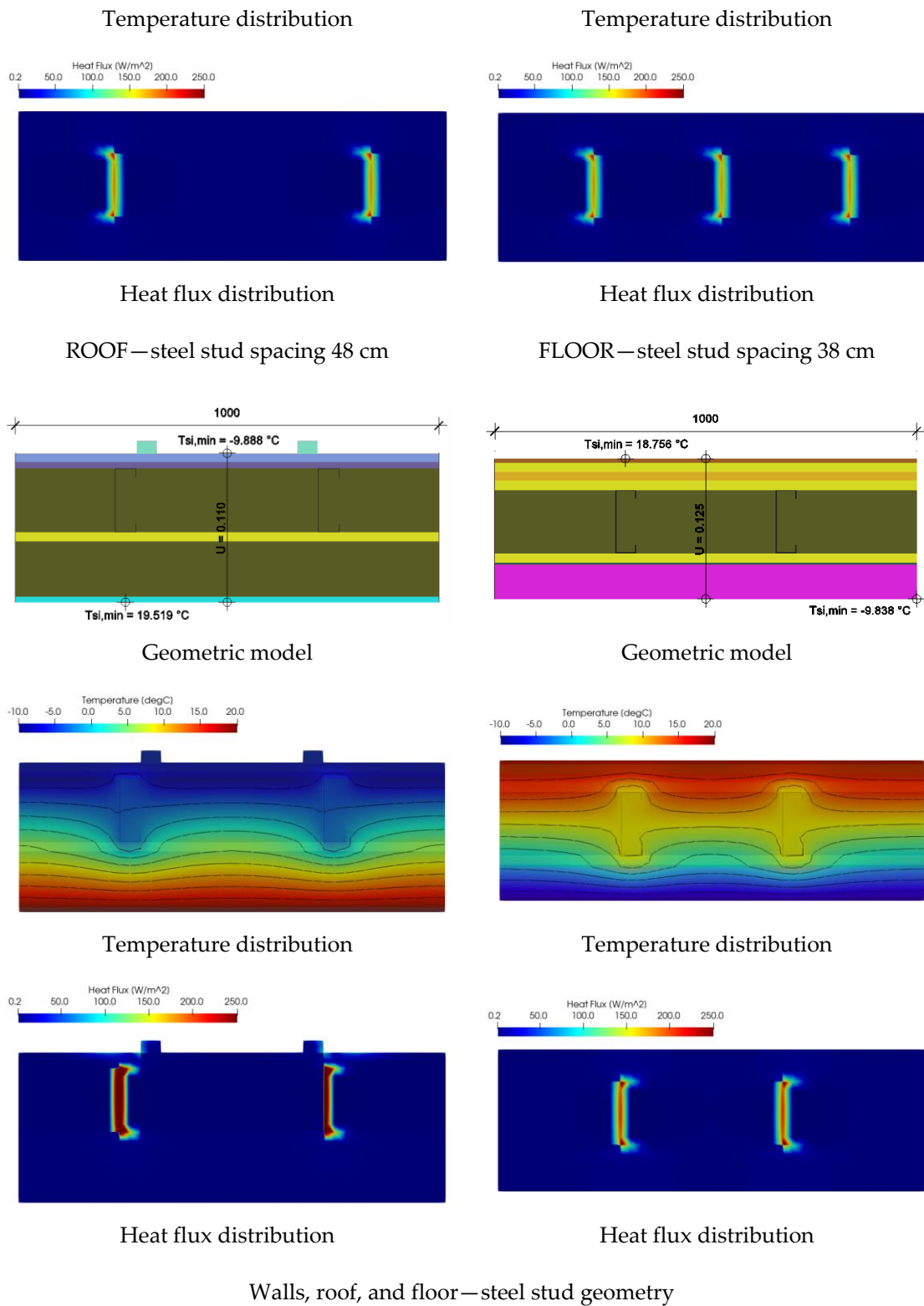
WALL—steel stud spacing 60 cm   WALL—steel stud spacing 30 cm

Geometric model   Geometric model

Figure 9. *Cont.*

Temperature distribution

Temperature distribution

Heat flux distribution

Heat flux distribution

ROOF—steel stud spacing 48 cm

FLOOR—steel stud spacing 38 cm

Geometric model

Geometric model

Temperature distribution

Temperature distribution

Heat flux distribution

Heat flux distribution

Walls, roof, and floor—steel stud geometry

Figure 9. *Cont*.

Figure 9. Model, temperature distribution, and heat flux.

Table 5. Results of the numerical models for the effective thermal transmittance calculation.

Building Element	Steel Stud Spacing [cm]	U_{eff} [W/(m² K)]	R_{eff} [m² K/W]	U [W/(m² K)]	R [m² K/W]	ΔU [%]	Ψ [W/(m K)]	f_{Rsi} [–]
Wall	60	0.14890	6.71592	0.116	8.62069	28.40	0.033	0.975
Wall	30	0.16429	6.08680	0.116	8.62069	41.60	0.048	0.975
Roof	48	0.14467	6.91228	0.110	9.09091	31.50	0.035	0.984
Floor	38	0.16534	6.04814	0.125	8	32.30	0.040	0.959

Numerical modelling resulted in significantly greater *U*-values when comparing the thermal performance of the walls with and without the steel studs (Table 5), with a discrepancy up to 28.4% and higher in the case of smaller stud spacing. The decrease in the steel stud spacing from 600 mm to 300 mm in the wall resulted in an increase in the U_{eff} of up to 41.6% compared to the *U*-value without the studs. Even though the increase was expected due to the increase in the number of steel studs per unit area of the wall, the magnitude of the increase is surprising. The heat flux distribution plots shown in Figure 9 illustrate the heat flux magnitude through the steel studs for the models analysed in this research.

It can be observed that, because the thermal insulation is placed on the external side of the LSF structure and is not penetrated by it, an effective thermal break is provided, without any continuous easy paths for heat flow to occur.

It is also evident from the results of the modelling (Table 5, Figure 9) that a comfortable environment can be guaranteed, since the thermal envelope resulted in temperatures as uniformly distributed over the internal surfaces as possible. This is evaluated by the f_{Rsi}, which is very close to indoor air (f_{Rsi} very close to 1). The resultant internal surface temperatures also have non-critical values regarding the appearance of mould growth or even condensation.

The MUZA's LSF walls can be considered a variant of hybrid frame construction, with additional continuous internal thermal insulation (in installation layer). The results presented in Table 5 indicate that the discrepancies in *U*-value (neglecting the steel frame by assuming homogeneous layers) and U_{eff}-value (walls with steel studs) are generally consistent with some similar studies found in the literature on hybrid frame construction. For instance, de Angelisa and Serra [28] concluded that only the interruption of the heat flow by an intermediate or external insulation layer (acting as a "thermal break") leads to a relevant limitation of the U_{eff} values. In their case, U_{eff} is about 25–30% higher than the baseline *U*-value when a greater insulation thickness of 12 cm is used for a hybrid wall with a steel stud spacing of 400–600 mm. It has also been confirmed in similar studies [23,45] that the main element responsible for improving the thermal performance of the walls is the continuous layer of external thermal insulation. The differences in the hybrid frame walls in these studies are up to 25.59% for different thermal insulation

thicknesses [23], and about 22% in [45]. On the other hand, in the study conducted by Moga et al. [16], these differences range from 38.83% to 53.67%, which is higher than the differences reported in Table 5. This can be attributed to the low thickness (22 mm) of the continuous external thermal insulation layer which Moga et al. [16] applied to their walls. The same authors [16] studied the effect of steel studs on the thermal transmittance of the flat roof and the ground floor above the crawl space, which resulted in significantly increased U_{eff}-values (ΔU = 100.80% for the roof and ΔU = 63.23% for the floor). A comparison with the corresponding values from Table 5 shows that these differences are much smaller in the case of the MUZA due to the different design approach (ΔU = 31.50% for the roof and 32.30% for the floor, respectively). In the case of the MUZA, the overall thermal performance of the hybrid floor is improved by the external polystyrene insulation layer, whose thickness is double that of [16], while the overall thermal performance of the roof is improved by the installation of a thick continuous internal thermal insulation and by the elimination of the air cavity between the steel studs. Consequently, the linear thermal transmittance ψ of the considered MUZA's components, as well as the condensation risk (reflected in the temperature factor f_{Rsi}), are also significantly lower.

Apart from the linear thermal bridges caused by the steel studs within the building elements, an additional type of thermal bridges can be recognised in LSF structure of the MUZA (namely external walls), which are point thermal bridges, usually driven by mechanical fixations (e.g., fixation of the mineral wool to the OSB as well as the substructure of the ventilated façade). In the case of the MUZA, the fixation of the mineral wool to the OSB sheeting is done using plastic fixings, and, as per EN ISO 6946 [34], can be ignored if thermal conductivity of the fastener is less than 1 W/(m K). Ventilated façade substructure is constructed using Crossfix consoles containing a plastic thermal break [46] with the calculated point thermal bridge coefficient χ = 0.0098 W/K and the ΔU = 0.0086 W/m²·K for the reference façade [47]. In addition to the plastic thermal break, the façade substructure consoles were screwed to the steel studs over the OSB sheeting, thus, additionally reducing the impact of the point thermal bridge. Consequently, it was concluded that the aforementioned point thermal bridges will be neglected in this research and will be analysed elsewhere.

5.2. MUZA's Thermal Bridges

Figure 10 visualizes the temperature distribution for the analysed construction details. The influence of steel elements (studs, beams, columns) on the temperature distribution is evident by strong concentration of the heat flux around steel.

Figure 10 and Table 6 give the results of the thermal bridges analyses.
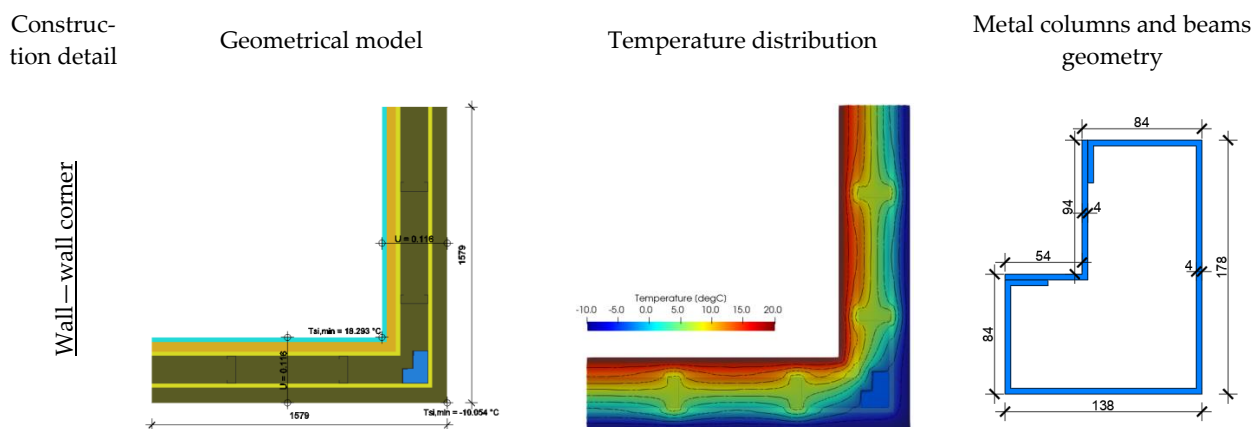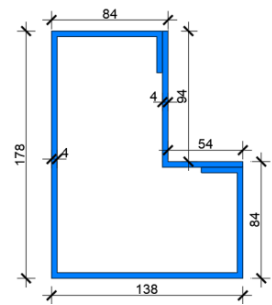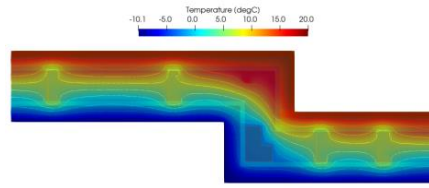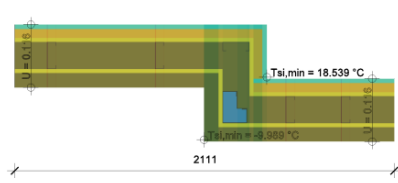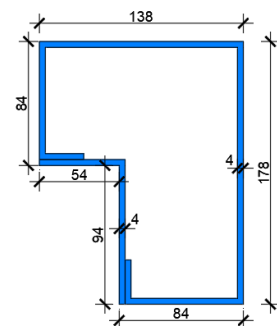

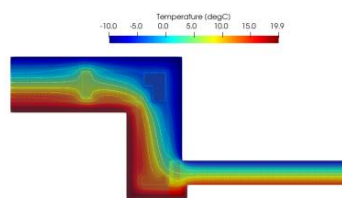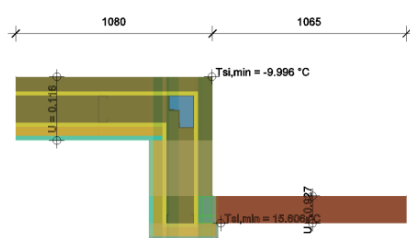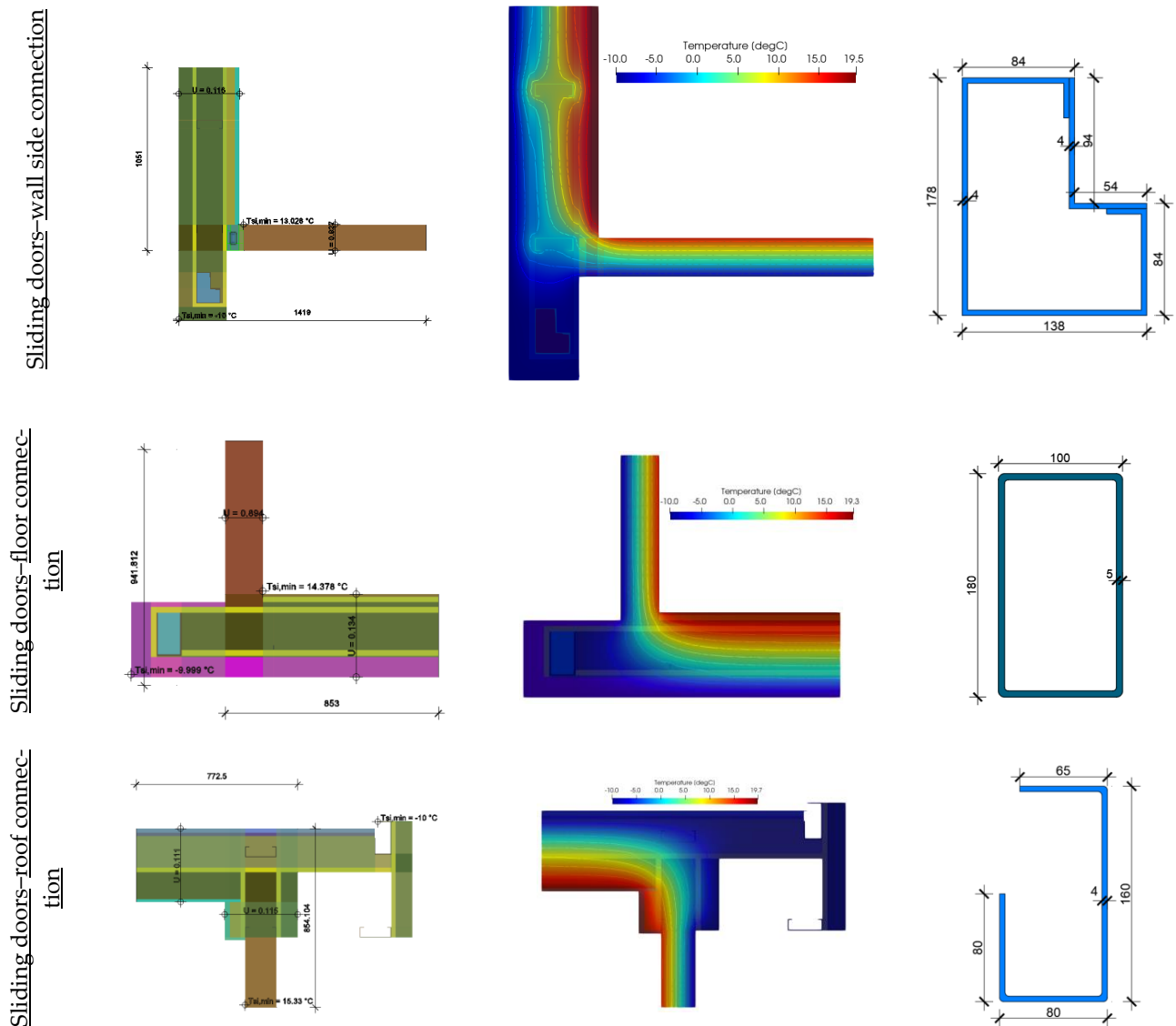**Figure 10.** *Cont.*
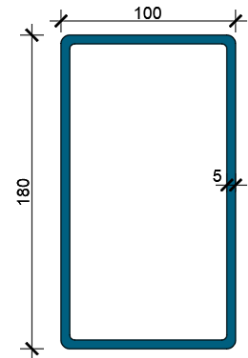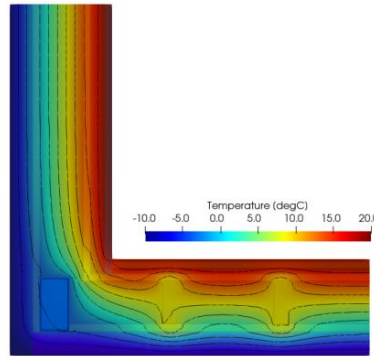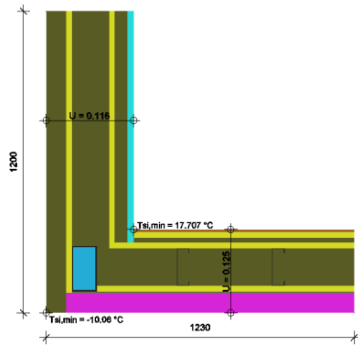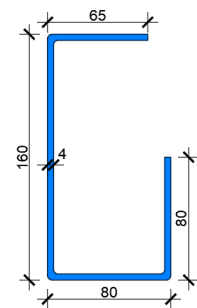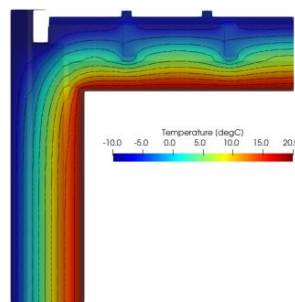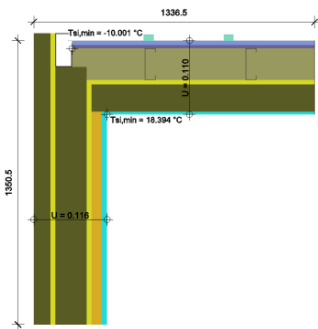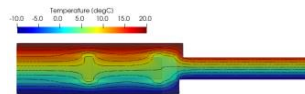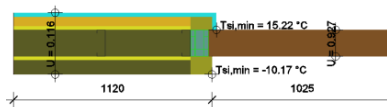
Figure 10. *Cont.*

Figure 10. Geometrical models and temperature distribution of the analysed thermal bridges.

Table 6. Results of numerical analysis of the analysed thermal bridges.

Construction Detail	L_{2D} [W/(m K)]	Ψ [W/(m K)]	Min. Surf. Temp. [°C]	f_{Rsi} [–]
Wall—wall corner	0.38410	0.0178	18.293	0.943
Wall—niche	0.32853	0.0800	18.539	0.951
Wall-floor connection	0.28919	−0.0038	17.707	0.924
Roof—wall connection	0.28417	−0.0195	18.394	0.946
Wall—sliding door frontal connection	1.14286	0.0628	15.220	0.841
Wall—sliding doors niche	1.22735	0.115	15.606	0.854
Sliding doors—wall side connection	1.22786	−0.209	13.028	0.768
Sliding doors—floor connection	0.69195	−0.295	14.378	0.813
Sliding doors—roof connection	0.40650	−0.472	15.330	0.844

The results (ψ-values) shown in Table 6 were calculated by using the U_{eff}-values from Table 5, while the internal surface temperatures were calculated for the geometry shown in Figure 10 with the real building's envelope layers and material properties. This approach was taken because the building's energy balance would presumably be calculated using the U_{eff} values due to the simplicity of the approach (accounting for the linear thermal bridges of steel studs directly in the U_{eff}), while the remaining thermal bridges should then be taken into account using the ψ-values calculated in Table 6.

It is evident from the results of the numerical calculations that wrapping the steel members of the LSF structure continuously with thermal insulation would contribute significantly to reduction in heat losses, with ψ-values well below 0.1 W/(m·K), except for the wall–sliding doors connection in the niche of the MUZA. This slightly worse value was because of the construction detail which, due to technological reasons and the slender sliding door frame, made it difficult to install additional external thermal insulation. Here, a relatively high internal surface temperature confirms that this version of the detail is also acceptable and there is no need to invest more resources into additionally reducing the ψ-value. The very low ψ-values obtained for the last three details in Table 6 are the consequence of the calculation procedure described above, as well as the use of U_{eff}.

While heat loss is a significant consequence of thermal bridging, the more potentially serious aspect results from the occurrence of low internal surface temperatures in thermal bridge areas. This can lead to surface condensation for non-absorbent materials or loss of thermal performance, structural integrity, and mould growth for absorbent materials.

Concerning the factor f_{Rsi}, it can be seen from Table 6 that the values are well above the limiting value of $f_{Rsi} = 0.7$, which ensures the reduced risk of mould growth on the internal surface of the considered construction details.

5.3. The Effect of Numerical Calculation of Thermal Bridges on the Energy Performance

The energy performance results using the conservative thermal bridge approach (default U-value increase by ΔU) are compared to the ones calculated using the ψ-values shown in Table 6 with respective lengths of thermal bridges together with U_{eff}-values of opaque envelope elements. The analysis was performed for the southern orientation of the main façade. Transmission heat losses H_D were the same for all climates (Table 7).

Table 7. Transmission heat losses H_D for the case of the MUZA.

	Units	Approach Using the Default U-Value Increase $\Delta U = 0.05$ W/(m^{2}K)	Approach Using the U_{eff} and Calculated ψ-Values	Relative Difference [%]
Total H_D	[W/K]	33.977	17.530	48.4
H_D—opaque building elements	[W/K]	21.429	16.189	24.5
H_D—transparent building elements	[W/K]	12.548	12.548	0.0
H_D—thermal bridges	[W/K]	0	−11.207	/

It can be seen from Table 7 that the total H_D were 48.4% lower for the case when calculations were performed using the calculated ψ-values and U_{eff}-values. The H_D value for opaque building elements was 24.5% higher when using the default U-value increase, which is a consequence of adding $\Delta U = 0.05$ W/(m^{2}K) to the U-values of the building envelope. As can be seen from Table 7, the contribution of thermal bridges to transmission heat losses is significant, where the negative value is due to the ψ-values calculation approach described above. Results indicate that using the default U-value increase can lead to unrealistically increased heat flow through building envelope elements, and, consequently, to increased energy demand on the whole building level. In such a way, the reliability of energy performance calculations can be questioned and lead to an increased energy performance gap (discrepancy between predicted and measured energy use), but this is out of the scope of this paper. On the other hand, applying U_{eff}-values and addressing 2D

heat flow more precisely describes the heat flow through the observed building envelope. Negative ψ-value has only a mathematical meaning; it does not represent an "opposite" heat flow direction. A negative ψ-value means that the actual heat flow is less than what was calculated using external measurements (external measurements are used to evaluate the whole thermal envelope).

Figure 11 gives the heating and cooling energy need calculations depending on the thermal bridge calculation approach (default *U*-value increase or calculated ψ-values and U_{eff}) for different climate conditions. It can be seen from Figure 11 that a significant decrease in $Q''_{H,nd}$ is achieved when calculated ψ-values and U_{eff}-values were used. This decrease was around 46% for the cooler climates of Gospić and Zagreb Maksimir, while for the warmer climates, the contribution was even higher (56.8% for Split Marjan and 58.5% for Hvar). On the other hand, as expected, the cooling energy need $Q''_{C,nd}$ has increased for all climates, to 28.9% and 20.6% for the cooler climates of Gospić and Zagreb Maksimir, respectively and 8.7% and 13.4% for warmer climates of Split Marjan and Hvar, respectively.

The total impact of thermal bridges on heating energy required is significant, while on the other hand, the impact on cooling energy, the relative conductive contribution of which is much smaller, is less significant. However, the impact on the cooling peak load might be significant.

Figure 12 shows that by taking into account the installed efficient heat pump and the PV system generating energy, the MUZA becomes a net-positive building, and the influence of the exact calculation of ψ-values of thermal bridges is also beneficial with regard to delivered and primary energy use. Again, larger influences of exact ψ-values are determined for the cooler climates. It must be mentioned here that these calculations of primary energy do not take into account embodied energy of the building, but only energy in use.
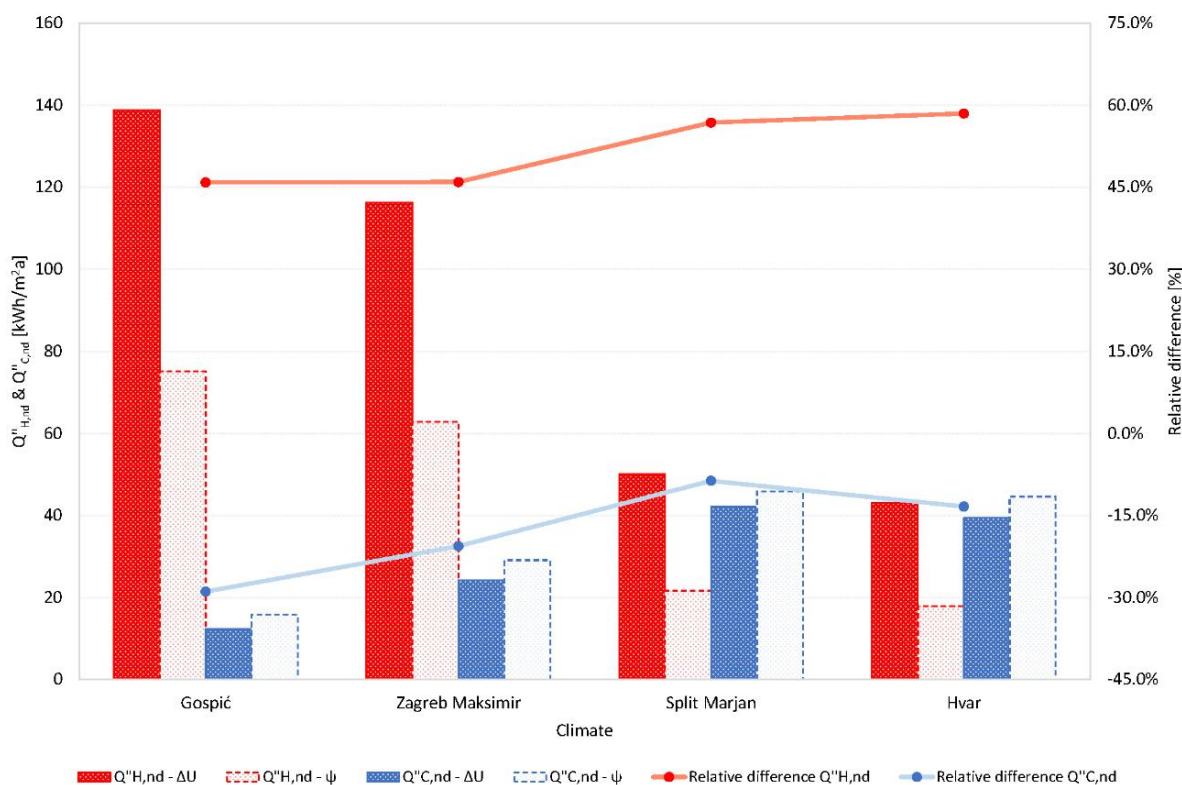

Figure 11. Heating and cooling energy needs depending on the thermal bridge consideration approach.

**Figure 12.** Delivered and primary energy use depending on the thermal bridge consideration approach.

According to Croatian technical regulations [14], there are maximum values defined as follows: $Q''_{H,nd}$ =75.00 kWh/m²a; $Q''_{C,nd}$ =50.00 kWh/m²a; E''_{prim} = 80.00 kWh/m²a for residential buildings in continental climates (Gospić and Zagreb Maksimir), while $Q''_{H,nd}$ =45.99 kWh/m²a; $Q''_{C,nd}$ =50.00 kWh/m²a; E''_{prim} = 50.00 kWh/m²a are defined maximum values for littoral climates (Split Marjan and Hvar). Comparing the maximum allowed values and the results from the Figures 11 and 12, it is evident not only that using calculated ψ-values would change the energy class of the building, but also that the specific building in question would fall under the NZEB requirements.

5.4. Climate and Orientation Effect on Energy Performance

Figure 13 gives the MUZA's energy needs for different locations in Croatia and relative differences with respect to Zagreb Maksimir for southern orientation of the main façade, all compared to the regulation requirements for NZEB for both continental and littoral climates (dashed lines). It can be seen that only the heating energy need $Q''_{H,nd}$ for Gospić is negligibly higher than the technical regulations demand, while for all other locations, it is well under the demanded values. The cooling energy need $Q''_{C,nd}$ complies with the regulations as well, even for the hottest city of Hvar. Due to the efficient heating and cooling system and PV system mounted on the roof of MUZA, E''_{del} and E''_{prim} are negative for all four climates, thus making the MUZA a net-positive building. One can see from Figure 13 that even though the heating energy need in Gospić is 19% higher than that of Zagreb Maksimir, the delivered energy for both of these cities is virtually the same (1% difference in favour of Gospić). This is due to the 46% lower cooling need in Gospić compared to Zagreb. In the cases of the littoral climates of Split Marjan and Hvar, both the delivered energy and the primary energy are significantly lower than in Zagreb Maksimir, which is due to the efficiency of the solar shading systems used, which reduce the cooling energy need.
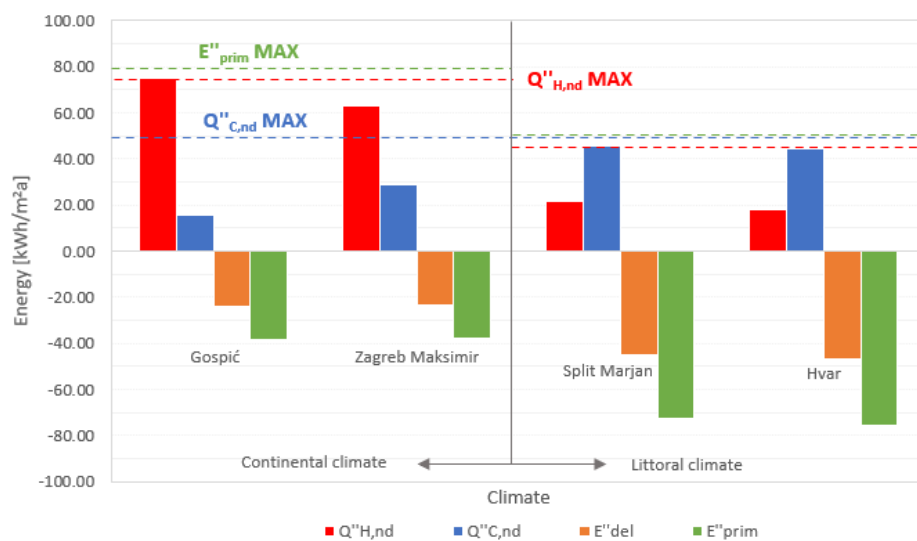
(**a**)
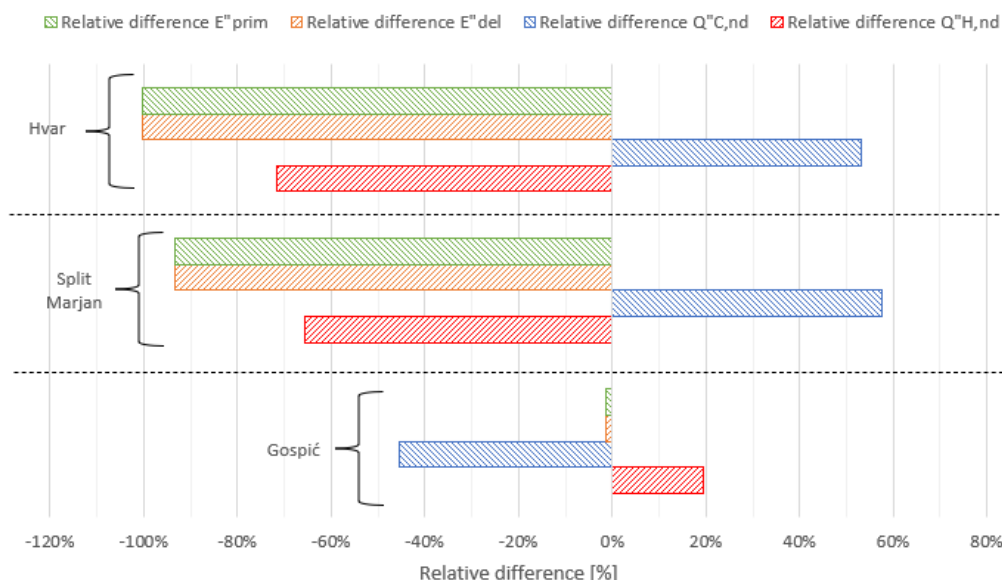
(**b**)

Figure 13. MUZA energy performance: (**a**) in different locations for southern orientation of the main façade; (**b**) relative differences in respect to the Zagreb Maksimir climate.

Orientation-dependent analysis was performed for the cases of the Zagreb Maksimir and Split Marjan climatic conditions, as representatives of the continental and littoral climates of Croatia for the four cardinal directions. Here, the main façade is the reference façade when analysing the building's orientation.

Figure 14 gives the MUZA energy needs for different orientations of the building's main façade, all compared to the regulation requirements for NZEB for both the continental and littoral climates (dashed lines). It can be seen that $Q''_{H,nd}$ and E''_{prim} are well under the maximum requirements of the regulations for both continental and littoral climates, for all orientations. It can be noted that the solar shading designed for MUZA worked well for the southern orientation, while it manifested significantly higher solar gains for other orientations. It can be noticed that for Split, eastern and western orientation caused a 45% increase in solar gains, while northern orientation resulted in 18% higher solar gains. This

in turn caused the $Q''_{C,nd}$ to exceed the regulation requirements for these three orientations in Split. The reasons for the increase in the case of eastern/western orientation can be found in the fact that the MUZA was not adequately protected from the incidence of energy during the lower sun positions in the east and west (morning and afternoon) during the entire year. The northern orientation resulted in an increase because of the smaller sliding doors on the back façade being freely exposed to the south solar gains, and the lack of textile overhang above these sliding doors. One can analyse the contribution of the overhang above the larger sliding doors on the main façade where it contributed to the decrease in the cooling energy need by 54%, and, in turn, the increase of heating energy needs by 17% in Zagreb Maksimir in the case of southern orientation, where the largest differences are noted. In the case of southern orientation in Split Marjan, it contributed to the decrease in $Q''_{H,nd}$ by 28% and the increase in the $Q''_{C,nd}$ by 39%. It is also evident from Figure 14 that the heat pump and PV system installed significantly reduce the delivered energy as well as the primary energy, making the MUZA a net-positive building in all orientations except north. This is due to the fact that PV orientation is fixed to the main façade orientation, and north is the most unfavourable orientation in the northern hemisphere for maximizing PV's exposure to direct sunlight. This could also be rectified by simple reorientation of the PV system on the roof, regardless of the orientation of the main façade.
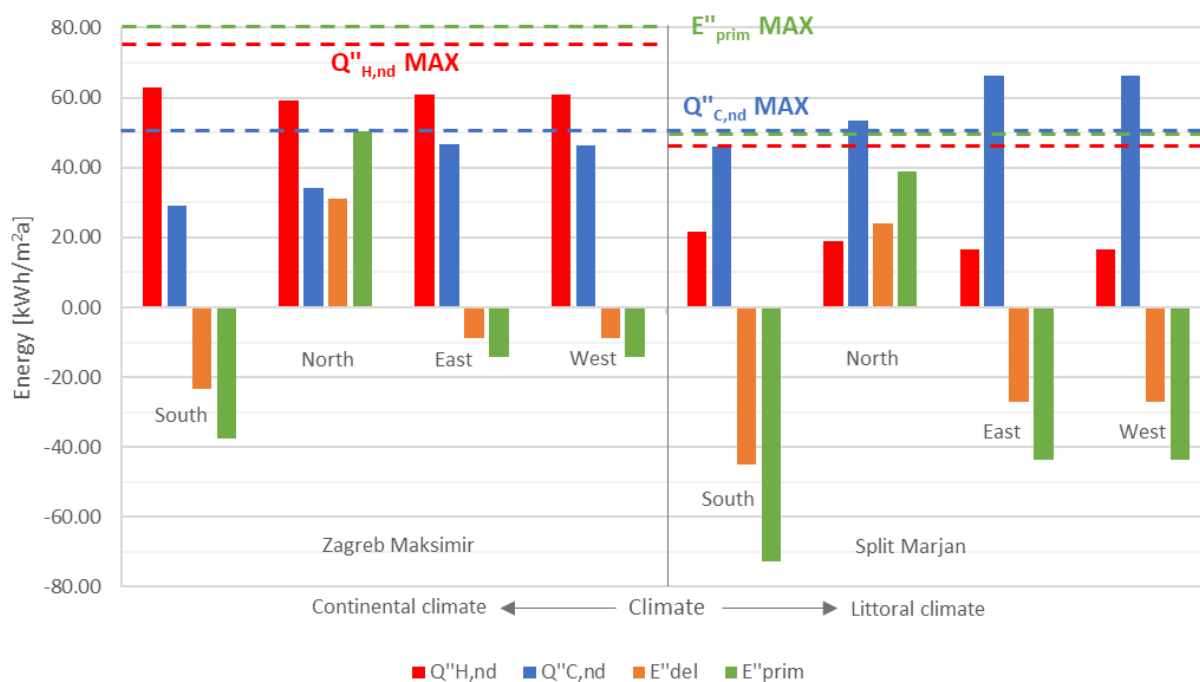

Figure 14. MUZA energy needs in respect to the main façade orientation.

6. Conclusions

This paper proposes the upgrading of a conventional Lightweight Steel Frame (LSF) structure, and presents a comprehensive assessment of the case study LSF building—the high-performance "MUZA" module, with a useful floor area of less than 50 m^2. Extensive analyses of the MUZA's performance were conducted, focusing on the effects of thermal bridging on energy performance and moisture condensation. Additional climate- and orientation-dependent analyses were performed in order to investigate how the module performed under different conditions.

From the presented results, it can be concluded that the suitable evaluation of thermal performances of LSF walls requires more complex and detailed analysis than those required for reinforced concrete or masonry structures. This means using numerical methods for calculating heat losses, including all steel studs and other construction details. It was shown in this research that the heterogeneity of structural and insulation materials, as well

as the high frequency of steel studs, lead to an underestimation of thermal transmittance if performing a *U*-value calculation for the case of one-dimensional heat flux.

It was also shown that applying thermal insulation on the outside of the steel frame (warm construction type), makes the most of its performance, leading to the reduction in the influence of steel elements on effective *U*-value to the minimum.

The superposition of thermal bridges along the entire building envelope certainly will create a considerable impact on the building's energy performance. In cases where an EU Member State's building code requires a default *U*-factor increase in buildings, for which calculations do not explicitly address thermal bridges, this value is usually found to be worse than if the thermal bridges had been explicitly calculated. That is, detailed calculation tends to predict a lower overall transmission heat loss for a building than does the addition of a default increment. This means that, because insulation improvements in the clear wall show diminishing returns, mitigating thermal bridges becomes the wiser investment. It was also shown in this research that the influence of the approach taken for including thermal bridges in the building's energy balance calculation also depends on the location of the building, where greater impact was shown on the heating energy need in the warmer climates.

Furthermore, it was shown in this research that by using LSF, it is possible to meet the Croatian requirements for NZEB buildings even for a building with a very small useful floor area, as observed in the presented case study. This means that for larger buildings constructed using two or more modules, as shown in this paper, it would be somewhat easier to achieve NZEB requirements. It was shown in this paper that by using an air-to-water heat pump and a small PV system mounted on the roof of the building, one can achieve net-positive building. A picture of the energy consumption of the module in different climates of Croatia and different orientations was gained by studying the MUZA, based on which one can draw design conclusions about using the LSF system for different building uses (from temporary buildings to permanent buildings).

In conclusion, the analysis presented in this paper broadens the knowledge about the possibilities and limitations of designing a LSF module by NZEB standards. The results indicate that the MUZA module is a promising solution for temporary (such as post-disaster housing) and permanent modular construction. However, this requires proof-of-concept. Hence, the future work will be focused on the constructed mobile pavilion MUZA and real-time monitoring of energy consumption, energy production, and different indoor air parameters (temperature, relative humidity, CO_2, and relative air quality), as well as hygrothermal performance of external walls. In situ measurements of the *U*-value will be performed and compared with numerically calculated values.

Nomenclature

A	External surface area of the building envelope	[m^2]
A$_f$	Gross floor area	[m^2]
A$_k$	Net floor area	[m^2]
A$_W$	Window surface area	[m^2]
COP	Coefficient of performance	[–]
d	Thickness of component layer	[m]
E$''_{del}$	Annual specific delivered energy	[kWh/(m^{2}a)]
E$''_{prim}$	Annual specific primary energy	[kWh/(m^{2}a)]
f$_P$	Primary energy factor	[-]
f$_{Rsi}$	Temperature factor	[-]
f$_0$	Shape factor	[m^{-1}]
g$_L$	The total solar energy transmittance (calculated for solar radiation perpendicular to the glazing)	[-]
h	Surface heat transfer coefficient	[W/(m^{2}K)]
H$_D$	Transmission heat losses	[W/K]
h$_{se}$	External surface heat transfer coefficient	[W/(m^{2}K)]
h$_{si}$	Internal surface heat transfer coefficient	[W/(m^{2}K)]
l	Length of the geometrical model	[m]
l$_i$	Length of the 2D geometrical model over which the Ui value is applied	[m]
L$_{2D}$	Two-dimensional thermal coupling coefficient	[W/(m·K)]
n	Number of specific layers in building component	[-]
n$_{50}$	Air changes per hour at a differential pressure of 50 Pa	[h-1]
P$_W$	Window perimeter	[m]
Q$''_{C,nd}$	Annual specific cooling energy need	[kWh/(m^{2}a)]
q$_{E50}$	Volume of air flowing through the m2 of envelope at 50 Pa pressure difference	[m^3/(h·m^2)]
Q$''_{H,nd}$	Annual specific heating energy need	[kWh/(m^{2}a)]
R	Thermal resistance	[(m^2·K)/W]
RH	Relative humidity	[%]
T	Temperature	[°C]
T$_i$	Internal environment (air) temperature	[°C, K]
T$_e$	External environment (air) temperature	[°C, K]
T$_{si,min}$	Minimum internal surface temperature	[°C, K]
U or U-value	Thermal transmittance of building envelope element	[W/(m^2·K)]
U$_{eff}$ or U$_{ef}$f-value	Effective thermal transmittance of opaque building envelope element	[W/(m^2·K)]
U$_f$	Thermal transmittance of frame	[W/(m^2·K)]
U$_g$	Thermal transmittance of glass	[W/(m^2·K)]
U$_i$	One-directional thermal transmittance of the i-th building element separating the two environments	[W/(m^2·K)]
U$_w$	Thermal transmittance of windows	[W/(m^2·K)]
V	Heated air volume	[m^3]
V$_e$	Heated building gross volume	[m^3]

Greek symbols

Δ	Difference between two quantities or increase of one quantity	[%] or [unit of observed quantity]
λ	Thermal conductivity of building material	[W/(m·K)]
μ	Water vapour diffusion resistance factor	[-]
φ	Heat flow rate (heat flux density divided by unit length)	[W/m]
χ	Point thermal bridge coefficient	[W/K]
Ψ	Linear thermal transmittance	[W/(m·K)]

References

1. Penna, A.; Morandi, P.; Rota, M.; Manzini, C.F.; da Porto, F.; Magenes, G. Performance of masonry buildings during the Emilia 2012 earthquake. *Bull. Earthq. Eng.* **2014**, *12*, 2255–2273. [CrossRef]
2. Mazzoni, S.; Castori, G.; Galasso, C.; Calvi, P.; Dreyer, R.; Fischer, E.; Fulco, A.; Sorrentino, L.; Wilson, J.; Penna, A.; et al. 2016–2017 Central Italy Earthquake Sequence: Seismic Retrofit Policy and Effectiveness. *Earthq. Spectra* **2018**, *34*, 1671–1691. [CrossRef]
3. Bilgin, H.; Shkodrani, N.; Hysenlliu, M.; Ozmen, H.B.; Isik, E.; Harirchian, E. Damage and performance evaluation of masonry buildings constructed in 1970s during the 2019 Albania earthquakes. *Eng. Fail. Anal.* **2022**, *131*, 105824. [CrossRef]
4. Vlachakis, G.; Vlachaki, E.; Lourenço, P.B. Learning from failure: Damage and failure of masonry structures, after the 2017 Lesvos earthquake (Greece). *Eng. Fail. Anal.* **2020**, *117*, 104803. [CrossRef]
5. Cetin, K.O.; Altun, S.; Askan, A.; Akgün, M.; Sezerm, A.; Kıncal, C.; Özkan, C.Ö.; İpek, Y.; Unutmaz, B.; Gülerce, Z.; et al. The site effects in Izmir Bay of October 30 2020, M7.0 Samos Earthquake. *Soil Dyn. Earthq. Eng.* **2022**, *152*, 107051. [CrossRef]
6. Stepinac, M.; Lourenço, P.B.; Atalić, J.; Kišiček, T.; Uroš, M.; Baniček, M.; Šavor Novak, M. Damage classification of residential buildings in historical downtown after the ML5.5 earthquake in Zagreb, Croatia in 2020. *Int. J. Disaster Risk Reduct.* **2021**, *56*, 102140. [CrossRef]

7. Milovanović, B.; Bagarić, M.; Gaši, M.; Stepinac, M. Energy renovation of the multi-residential historic building after the Zagreb earthquake–Case study. *Case Stud. Therm. Eng.* **2022**, *38*, 102300. [CrossRef]

8. Croatian Centre of Earthquake Engineering Assessment Results by County 10 May 2021. Available online: https://www.hcpi.hr/sites/default/files/2021-05/2021%05%11%sredeno%(PNG).png (accessed on 28 September 2022). (In Croatian).

9. Government of the Republic of Croatia and the World Bank. *The Croatia Earthquake-Rapid Damage and Need Assessment 2020*; Government of the Republic of Croatia: Zagreb, Croatia, 2020.

10. Perković, N.; Stepinac, M.; Rajčić, V.; Barbalić, J. Assessment of Timber Roof Structures before and after Earthquakes. *Buildings* **2021**, *11*, 528. [CrossRef]

11. Večernji List the Investigation in Glina Has Been Completed, the Cause of the Container Fire Is Known. Available online: https://www.vecernji.hr/vijesti/zavrsen-ocevid-u-glini-poznat-uzrok-pozara-kontejnera-1562064 (accessed on 28 September 2022). (In Croatian).

12. Paparella, R.; Caini, M. Sustainable Design of Temporary Buildings in Emergency Situations. *Sustainability* **2022**, *14*, 8010. [CrossRef]

13. European Parliament and the Council. *Directive 2010/31/EU of the European Parliament and of the Council of 19 May 2010 on the Energy Performance of Buildings (Recast)*; European Parliament: Luxembourg, 2010; p. OJEU L153/13.

14. Ministry of Physical Planning Construction and State Asset Technical regulation on energy economy and heat retention in buildings. *Official Gazzete 128/15, 70/18, 73/18, 86/18, 102/20*, 16 September 2020. (In Croatian)

15. European Commission. *Proposal for a Directive of the European Parliament and of the Council on the Energy Performance of Buildings (Recast)*; European Commission: Brussels, Belgium, 15 December 2021.

16. Moga, L.; Petran, I.; Santos, P.; Ungureanu, V. Thermo-Energy Performance of Lightweight Steel Framed Constructions: A Case Study. *Buildings* **2022**, *12*, 321. [CrossRef]

17. Açıkkalp, E.; Kandemir, S.Y. A method for determining optimum insulation thickness: Combined economic and environmental method. *Therm. Sci. Eng. Prog.* **2019**, *11*, 249–253. [CrossRef]

18. Rodrigues, E.; Soares, N.; Fernandes, M.S.; Gaspar, A.R.; Gomes, Á.; Costa, J.J. An integrated energy performance-driven generative design methodology to foster modular lightweight steel framed dwellings in hot climates. *Energy Sustain. Dev.* **2018**, *44*, 21–36. [CrossRef]

19. Santos, P. Energy Efficiency of Lightweight Steel-Framed Buildings. In *Energy Efficient Buildings*; Yap, E.H., Ed.; InTech: London, UK, 2017.

20. Liang, H.; Roy, K.; Fang, Z.; Lim, J.B.P. A Critical Review on Optimization of Cold-Formed Steel Members for Better Structural and Thermal Performances. *Buildings* **2022**, *12*, 34. [CrossRef]

21. Mihić, F.; Markulak, D.; Dokšanović, T. Use of structural steel in residential construction. *J. Croat. Assoc. Civ. Eng.* **2022**, *74*, 419–431. [CrossRef]

22. Brito-Peña, R.; Villa-Enderica, D.; Zalamea-León, E. Análisis comparativo de confort térmico de vivienda unifamiliar en LSF frente a mampostería. *Ingenius* **2022**, *28*, 100–124. [CrossRef]

23. Roque, E.; Santos, P. The Effectiveness of Thermal Insulation in Lightweight Steel-Framed Walls with Respect to Its Position. *Buildings* **2017**, *7*, 13. [CrossRef]

24. Olivieri, H.; Barbosa, I.C.A.; da Rocha, A.C.; Granja, A.D.; Fontanini, P.S.P. A utilização de novos sistemas construtivos para a redução no uso de insumos nos canteiros de obras: Light Steel Framing. *Ambient. Construído* **2017**, *17*, 45–60. [CrossRef]

25. European Commission. *Communication from the Commission to the European Parliament, the European Council, the Council, the European Economic and Social Committee and the Committee of the Regions—The European Green Deal*; European Commission: Brussels, Belgium, 2019; Available online: https://eur-lex.europa.eu/resource.html?uri=cellar:b828d165-1c22-11ea-8c1f-01aa75ed71a1.0002.02/DOC_1&format=PDF (accessed on 5 September 2022).

26. European Commission. *ANNEX to the Communication from the Commission to the European Parliament, the European Council, the Council, the European Economic and Social Committee and the Committee of the Regions—European Green Deal*; European Commission: Brussels, Belgium, 2019; Available online: https://eur-lex.europa.eu/resource.html?uri=cellar:b828d165-1c22-11ea-8c1f-01aa75ed71a1.0002.02/DOC_2&format=PDF (accessed on 5 September 2022).

27. Samani, P.; Leal, V.; Mendes, A.; Correia, N. Comparison of passive cooling techniques in improving thermal comfort of occupants of a pre-fabricated building. *Energy Build.* **2016**, *120*, 30–44. [CrossRef]

28. de Angelis, E.; Serra, E. Light Steel-frame Walls: Thermal Insulation Performances and Thermal Bridges. *Energy Procedia* **2014**, *45*, 362–371. [CrossRef]

29. Roque, E.; Vicente, R.; Almeida, R.M.S.F.; Ferreira, V.M. The Impact of Thermal Inertia on the Indoor Thermal Environment of Light Steel Framing Constructions. *Energies* **2022**, *15*, 3061. [CrossRef]

30. Jelčić Rukavina, M.; Skejić, D.; Kralj, A.; Ščapec, T.; Milovanović, B. Development of Lightweight Steel Framed Construction Systems for Nearly-Zero Energy Buildings. *Buildings* **2022**, *12*, 929. [CrossRef]

31. The nZEB Roadshow Horizon 2020 Project "The nZEB Roadshow". Available online: https://www.nzebroadshow.eu/ (accessed on 26 August 2022).

32. Faculty of Civil Engineering University of Zagreb Mobile NZEB Pavillion MUZA. Available online: https://www.muza-nzeb.com/ (accessed on 26 August 2022). (In Croatian).

33. Maxwell, S. Why We Should Change Our Building Air Tightness Metrics. Available online: https://thefifthestate.com.au/columns/spinifex/why-we-should-change-our-building-air-tightness-metrics/ (accessed on 24 August 2022).

34. *EN ISO 6946:2017*; Building Components and Building Elements–Thermal Resistance and Thermal Transmittance–Calculation Methods. The European Committee for Standardization: Brusels, Belgium, 2017.

35. *EN ISO 10211:2017*; Thermal Bridges in Building Construction—Heat Flows and Surface Temperatures—Detailed Calculations. The European Committee for Standardization: Brusels, Belgium, 2017.

36. *EN ISO 14683:2017*; Thermal Bridges in Building Construction—Linear Thermal Transmittance—Simplified Methods and Default Values. The European Committee for Standardization: Brusels, Belgium, 2017.

37. Schild, K. *Wärmebrücken-Berechnung und Mindestwärmeschutz*; Springer Fachmedien Wiesbaden: Wiesbaden, Germany, 2018; ISBN 978-3-658-20708-3.

38. Gorgolewski, M. Developing a simplified method of calculating U-values in light steel framing. *Build. Environ.* **2007**, *42*, 230–236. [CrossRef]

39. ASHRAE Building Envelope, Chapter 25. "Heat, Air, and Moisture Control in Building Assemblies–Fundamentals" and Chapter 27. "Heat, Air, and Moisture Control in Building Assemblies–Examples". In *Handbook of Fundamentals*, SI ed.; ASHRAE—American Society of Heating, Refrigerating and Air-Conditioning Engineers: Atlanta, GA, USA, 2017; p. 1014.

40. Gaši, M. *CRORAL-Computer Program for Thermal Bridge Analysis and Vapour Analysis*; University of Zagreb, Faculty of Civil Engineering: Zagreb, Croatia, 2021.

41. *EN ISO 10077-2:2017*; Thermal Performance of Windows, Doors and Shutters—Calculation of Thermal Transmittance—Part 2: Numerical Method for Frames. The European Committee for Standardization: Brusels, Belgium, 2017.

42. Hens, H. *Performance Based Building Design 1*, 2nd ed.; Wiley-VCH Verlag GmbH & Co. KGaA: Weinheim, Germany, 2012; ISBN 9783433601952.

43. *EN ISO 13790:2008*; Energy Performance of Buildings–Calculation of Energy Use for Space Heating and Cooling. The European Committee for Standardization: Brusels, Belgium, 2008.

44. Lončar, D.; Dović, D.; Horvat, I. *Algorithm for Determining Energy Requirements and Efficiency of Thermotechnical Systems in Buildings-Cogeneration Systems, District Heating Systems, Photovoltaic Systems*; University of Zagreb, Faculty of Mechanical Engineering and Naval Architecture: Zagreb, Croatia, 2017. (In Croatian)

45. Santos, P.; Lemes, G.; Mateus, D. Thermal Transmittance of Internal Partition and External Facade LSF Walls: A Parametric Study. *Energies* **2019**, *12*, 2671. [CrossRef]

46. ETA-Danmark A/S. *European Technical Assessment ETA-21/0756 of 2021/09/03*; ETA-Danmark A/S: Copenhagen, Denmark, 2021.

47. Passive House Institute. *EJOT Wandwinkelstütze-Certified Passive House Component for Cool, Temperate Climate*; Passive House Institute: Darmstadt, Germany, 2022.